ECO-FRIENDLY DRIVEN REMEDIATION OF THE INDOOR AIR ENVIRONMENT: THE SYNTHESIS OF NOVEL TRANSITION METAL DOPED TITANIA/SILICA AEROGELS FOR DEGRADATION OF VOLATILE AND SEMI-VOLATILE ORGANIC COMPOUNDS

by

SCHUYLER DENTON BAKER

B.S., Benedictine College, 2008

A THESIS

submitted in partial fulfillment of the requirements for the degree

MASTER OF SCIENCE

Department of Chemistry
College of Arts and Sciences

KANSAS STATE UNIVERSITY
Manhattan, Kansas

2012

Approved by:

Major Professor
Dr. Kenneth Klabunde

Copyright

Abstract

Remediation of the indoor environment led to the development of novel catalysts which can absorb light in the visible range. These catalysts were prepared using the wet chemistry method known as sol-gel chemistry because preparation via sol-gel provides a homogeneous gel formation, which can be treated via supercritical drying to produce an aerogel. These aerogels have been found to have high surface areas when a combination of titania/silica is used. The increase in surface area has been shown to enhance the activity of the catalysts. Mixed metal oxide systems were prepared using titanium isopropoxide and tetraethyl orthosilicate to yield a 1:1 system of titania/silica (TiO_2/SiO_2). These systems were doped during the initial synthesis with transition metals (Mn or Co) to create mixed metal oxide systems which absorb light in the visible light range. These materials were assessed for potential as heterogeneous catalysts via gas-solid phase reactions with acetaldehyde. Degradation of acetaldehyde as well as the formation of CO_2 was monitored via gas chromatography-mass spectrometery. To increase the activity, visible light was introduced to the system. Experiments have shown that a 10 mol % manganese doped titania/silica system, in the presence of light, can degrade acetaldehyde. The cobalt doped counterpart showed dark activity in the presence of acetaldehyde resulting in the formation of CO_2 without the addition of visible light. In the hope of increasing surface area a mixed solvent (toluene/methanol) synthesis procedure was applied to the manganese doped catalyst. The resulting materials were of a low surface area but showed a significant increase in degradation of acetaldehyde.

Examination of the interactions between mixed metal oxide systems and semivolatile organic compounds (SVOCs) was studied. The pollutant, triphenyl phosphate, was dissolved in n-pentane and exposed to 10 mg of a given catalyst. These reactions were monitored using UV-Vis. All systems but the manganese doped titania/silica system resulted in the observation of no activity with triphenyl phosphate. The manganese doped catalyst shown a peculiar activity, the increase in absorbance of the triphenyl phosphate peaks as well as the formation of a new peak.

Table of Contents

List of Figures

List of Tables

Acknowledgements

I would like to thank Dr. Kenneth Klabunde for accepting the role as my graduate advisor and for his patience and perseverance throughout my graduate career. The warm welcoming and hospitality of Dr. Klabunde and his wife Linda Klabunde help to form a foundation of friendship throughout the group. I would also like to thank Dr. Kennedy Kalebaila, the post doc during my first year, for his inspiration and guidance during my summer research assistantship and first year as a graduate student. It was his guidance that shaped the foundation of my experience at Kansas State University. I would also like to thank Jackie Johnson, the summer REU student, who I had the pleasure of working with. Lastly, I would like to thank all the Klabunde group members without their advice and mentorship I would not have been able to achieve the work I have. I would also like to thank the Target of Excellence for their funding which allowed for the completion of this research.

Chapter 1 - Synthesis and Modification of Novel Eco-Friendly Manganese Doped Titania/Silica Catalyst: Photoactive to Dark Active

1.1 Introduction

The primary goal of our research was to develop novel materials for use in remediation of the indoor air environment. We will therefore begin with an overview of indoor air pollution. In the home, air pollution occurs from the release of gases and particles into the air. If there is not enough ventilation the problem becomes even worse due to the lack of air flow into the home to dilute these pollutants as well as the lack of diffusion of air out of the home carrying the pollutants away. Certain pollutants can be increased in concentrations due to high temperatures and humidity levels. Some common sources of indoor air pollution [1,2,3,4,5] are: combustion of oil, gas, kerosene, coal, wood and tobacco products, asbestos, household cleaning and personal care products, pesticides and outdoor air pollution. Any of these sources can cause a wide range of adverse health effects. There can be short term such as irritation of the eyes, nose, and throat, dizziness, fatigue or headaches, which are often treatable. They can also be long-term effects such as respiratory disease, heart disease, cancer and other effects that can be severely debilitating or even fatal. This information provides an overview of all air pollution which can occur in the indoor environment. For the purpose of environmental remediation research, the entire spectrum of pollution is too overwhelming. We therefore narrowed the scope to pollutants of a nature easy to work with in the lab. For this reason we choose volatile organic compounds, VOCs.

According to the EPA volatile organic compounds are gases which evolve from certain solids or liquids. These gases can have many varying adverse health effects such as headache, nausea,

loss of coordination, as well as, damage to the liver, kidney, and central nervous system.[6] These gases can be formed by many common materials found inside such as asbestos, household cleaning products, personal care products, and even from the burning of hydrocarbons. Certain studies have shown that the concentration level of several organics the can be found inside homes are two to five times higher than outdoors.[6] Over the last few decades we have come to realize that pollution to the environment and to us is harmful and have taken steps to reduce emission but general perception is often limited only to the outdoors. Now days, it is more common for an individual to spend the majority of their workday inside. It is therefore important that we change our way of thinking to a more global recognition of pollution both in the environment outside and in our growing indoor world.

1.2 Previous Methods of Remediation

To tackle this task of air remediation, we begin by examining previous methods. One method for removing gases from an environment is using adsorption, such as activated carbon.[7] This method relies of high surface area materials to trap the pollutant but this method does not solve the problem. In fact, in some ways it creates a greater one by concentrating the pollutant.

Another method is the use of chemical oxidation to destroy the pollutant. This method requires often toxic materials such as permanganates[8] and persulfates which can be fairly expensive and typically are not very robust. Our aim is to establish novel methods for air remediation that are both inexpensive and destructive. One such method could be the use of photocatalysis. One material that would be well suited for this purpose is titanium dioxide.

1.3 Promising Catalyst: Titania

In the 1970's a Japanese group of scientists published an article in Nature that showed how water could be split via electrolysis using titanium dioxide and platinum as electrodes.[9] Water can only

be decomposed by direct irradiation of light with wavelengths less than 190 nm.[9] Electrochemical decomposition of water can occur when a potential difference > than 1.23 eV is applied between electrodes which correlates to irradiation energy of ~ 1,000 nm. For this reason, Honda and Fujishima worked to design a photo-electrochemical cell that could use irradiation rather than an applied voltage to decompose water. Titanium dioxide was the material of choice because of its band gap ~3.0 eV. Using titanium dioxide and platinum as electrodes, they succeeded in producing hydrogen and oxygen from water.

Titania based catalysts have become increasingly important due to their activity at room temperature, inert, nontoxic and the nature of their band gaps. It is for these reasons that titania was chosen to be used as the base for developing novel catalysts for environmental remediation. Titania (TiO_2) has a band gap between 3.0-3.2 eV depending on the crystalline phase. The catalysts synthesized in this paper utilize anatase phase titania, band gap 3.2 eV, because of known photo-activity in the ultraviolet range (387.5 nm) and low heat treatment.[10,11] Although being ultraviolet light active is a start UV light only accounts for ~ 5% of the solar energy and is dangerous to be exposed to constantly in an enclosed space. Therefore the goal is to use dopants that shift the band gap into the visible light absorbing region. This has been achieved using many different dopants: carbon[11,12,13], sulfur[11], nitrogen[14] and more recently transition metals.[11,13,15] In attempts to improve the activity of the catalyst, it has been found that increasing the surface area can lead to an increase in the absorption and degradation of pollutants.[16, 17] To increase the surface area titania is mixed with silica which allows for an increase in the surface area without excessive changes in the overall activity of the catalyst and in some cases even enhances the activity.

1.4 Modified Sol-Gel Method

When deciding on the method of preparation for a catalyst it is important to know what advantages a given method provides. Perhaps one of the most important properties of the sol-gel method is it produces homogenous gels. The development of our manganese catalysts are based on a wet chemistry method known as sol-gel chemistry.[18,19] Sol-gel refers to the formation of a gel structure from an aqueous solution. The basic principles of the sol-method can be found in **Figure 1-1**. A more in depth look at the sol-gel method finds there are five steps to the process as used in this experiment:

i. Formation of sol from precursors
ii. Gelation of the sol via the formation of an oxide or alcohol bridged networks
iii. Aging of the gel, also known as synersis, during which polycondensation reactions continue to occur until lack of precursors
iv. Drying of the gel
    a. Open container evaporation of the solvent- Xerogel
    b. Supercritical drying via autoclave in a pressured system- Aerogel
v. Densification of the powder gel via heat treatment at 500 °C for 2 hours.

To begin, metal salts or metal alkoxides are dissolved in a solvent, usually an alcohol to reduce side products. A common metal alkoxide precursor is tetraethyl orthosilicate, $Si(OEt)_4$. This precursor is this subjected to hydrolysis producing a colloidal suspension known as the sol. Colloids are solid particles of diameters ranging from 1-100 nm.

The sol is comprised of discrete nanoparticles suspended in solvent, which upon condensation yields a wet gel with solid strings of nanoparticles with liquid solvent filling the pores. There are two options for treatment each producing a unique type of gel: bench top drying yields a xerogel

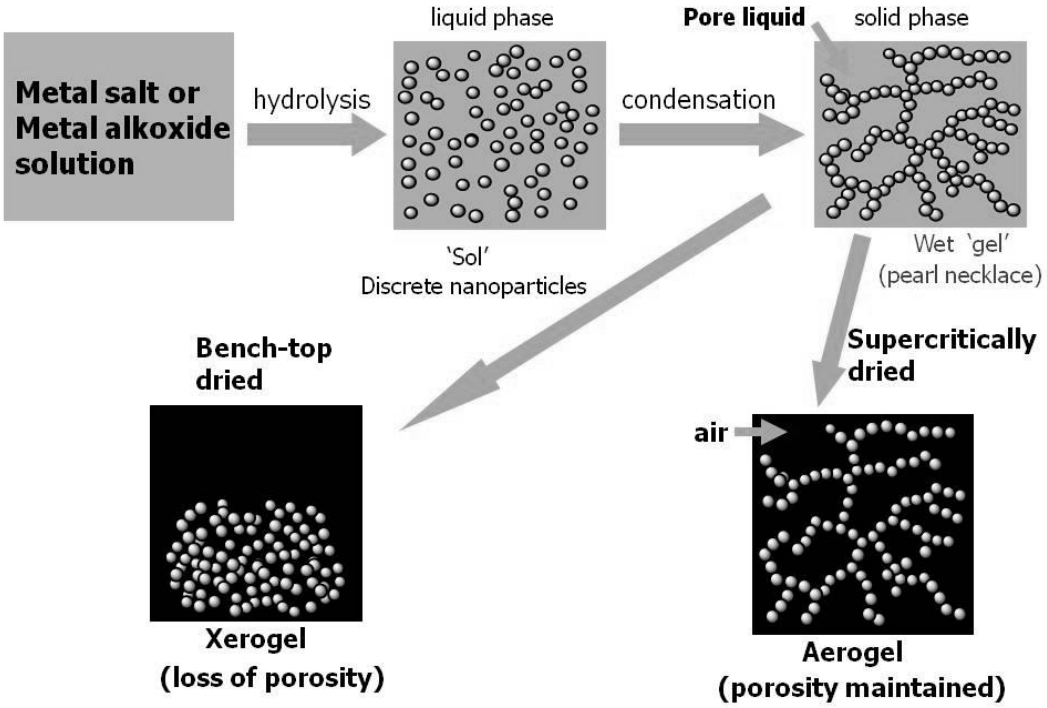

Figure 1-1 This model represents the basic steps in the sol-gel method. Metal salts or alkoxides undergo hydrolysis to produce a sol. This sol then under goes condensation to produce a wet "gel". This gel can then be treated one of two ways to produce either a xerogel or an aerogel.

which typically have a larger particle size and lower surface area or supercritical drying that yields a high surface area and smaller average particle size aerogel. The difference in the two arises from the method in which the solvent is removed. During drying for xerogels, the pores collapse in on themselves due to the surface tension of the solvent. Aerogels' solvent is removed above the supercritical temperature for the given solvent causing the solvent to evaporate out of the pores without causing a disruption in the pore size and shape.

There are several key points to take away from this method of synthesis first of which is the choice of precursors which can be used to create a gel are vast. Between the formation of the sol

and the gel there is a period in which the material can be cast into a mold if a given shape is desired of the ending gel. In order to prevent adhesion of the gel the mold into which the gel is cast must be selected specifically for the particular chemical composition. Aging of a gel is important for developing the strength needed to prevent cracking during drying. During the aging process polycondensation also continues to occur locally within the gel causing an increase in the thickness of the particle structure and a decrease in the porosity.

1.5 Synthesis of Titania/Silica Gels

Titania-silica aerogels were prepared by dissolving 24.1 mL of tetraethyl orthsilicate (TEOS) in 186 mL of ethanol and 14 mL of ethyl acetoacetate. This solution was stirred vigorously as 32.1 mL of $Ti(O^iPr)_4$, titanium isopropoxide, was added slowly to the solution. This solution labeled, solution one, was allowed to stir for ten minutes while solution two was prepared. Solution two was prepared by dissolving 3.8 g of manganese (III) acetyl acetonate in 20 mL of ethanol and was then allowed to stir for ten minutes to ensure all manganese (III) acetyl acetonate dissolved. After stirring solution two was added to solution one and the flask rinsed with a small amount of ethanol to remove any remaining manganese (III) acetyl acetonate. This solution was then allowed to stir for 10 minutes while a solution of NH_4OH/H_2O (3.7 mL/23.4 mL respectively) was prepared. The NH_4OH/H_2O was then added slowly drop wise to the solution and para filmed to prevent evaporation. The flask was left stirring for a period of 24 hours to allow for the formation of a gel. **Figure 1-2** shows the change in appearance of solution for a given step.

Preparation of mixed solvent systems followed similar procedures as above with some minor differences. Preparation began by dissolving 6 mL (0.027 mmol) of tetraethyl orthsilicate (TEOS) in 46.5 mL of methanol and 3.5mL of ethyl acetoacetate. This solution was stirred vigorously as 8.025 mL (0.027 mmol) of $Ti(O^iPr)_4$, titanium isopropoxide, was added slowly to

the solution. This solution labeled, solution one, was allowed to stir for ten minutes while solution two was prepared. Solution two was prepared by dissolving 0.95 g of manganese (III) acetyl acetonate in 10 mL of methanol/3.5 mL ethyl acetoacetate and was then allowed to stir for ten minutes to ensure all manganese (III) acetyl acetonate dissolved. After stirring solution two was added to solution one and the flask rinsed with a small amount of ethanol to remove any remaining manganese (III) acetyl acetonate. This solution was then allowed to stir for 10 minutes while a solution of NH_4OH/H_2O (0.925 mL/5.57 mL respectively) was prepared. The NH_4OH/H_2O was then added very slowly drop wise to the solution to prevent precipitation. Upon completing the addition of NH_4OH/H_2O the flask was then para filmed to prevent evaporation. The flask was left stirring for a period of 24 hours to allow for the formation of a gel and a consistent aging period. Three more gels were prepared using this method exchanging pure methanol for a toluene/methanol ratio of 0.8, 1.6 and 1.96.

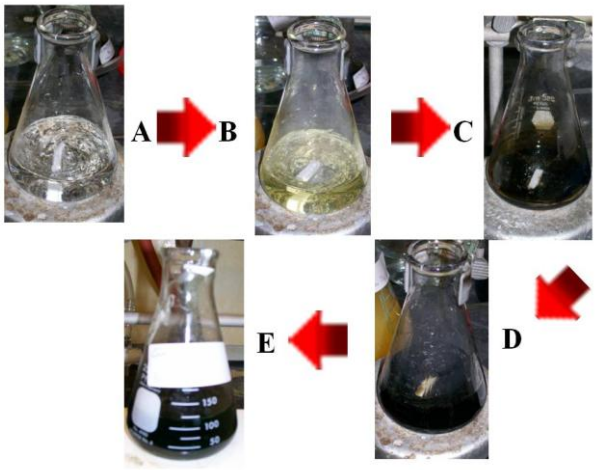

Figure 1-2 A) A solution containing methanol ethyl aceto acetate and $Si(OEt)_4$. B) Upon the addition of $Ti(O^iPr)_4$ the solution turns yellow temporarily as the ethyl acetoacetate reacts with the titanium. C) The addition of manganese (III) acetyl acetonate yields a dark purple solution. D) After the addition of NH_4OH/H_2O the solution begins to gel. E) Within minutes the gel has solidified.

1.6 Characteristics

Powder X-ray diffraction (PXRD) was used to identify the crystallite phase present in titania/silica doped aerogels. PXRD data was obtained using a Scintag XDS 200D8 diffractometer equipped with a copper anode with a Kα radiation of wavelength of 0.15406 nm from 2-75° (2θ). Samples were prepared for PXRD study by spreading a small amount of powdered aerogel onto a quartz background plate. Particle size was approximated using the Scherer equation based on the PXRD diffraction patterns.

The Brunauer-Emmett-Teller (BET) surface area and the Barret-Joyner-Halenda (BJH) pore size distribution of the doped aerogels were obtained from nitrogen adsorption/desorption isotherms using a 30 sec equilibrium interval on a NOVA 1000 series Quantachrome Instrument acquired at 77 K. The samples were degassed to remove any adsorbed molecules at 100 °C over night prior to analysis.

Solid state UV-Vis absorption was studied using a CARY 500 UV/VIS/NIR spectrophotometer equipped with an integrating sphere between wavelengths of 200-800 nm. The instrument was calibrated using a light reflecting powder as a reference (1 micron polytetrafluoroethylene).

Electron Spin Resonance (ESR) spectra were collected using a Bruker EMX spectrometer equipped with an ER041XG microwave bridge at a frequency of 9.34 GHz and power of 2.02mW at 77 k to determine the active species of manganese in doped titania/silica aerogels.

1.7 Photocatalysis

Photocatalytic degradation experiments were carried out in a cylindrical glass reactor consisting of a total volume of 305 mL and a quartz glass window shown in **Figure 1-3**. A circular glass stand was used to station the powdered aerogels away from the liquid acetaldehyde with a magnetic stir bar under the stand. A typical experiment consisted of placing 100 mg of a given

powdered aerogel in the stand and injecting 100 µL of liquid acetaldehyde (CH_3CHO) into a side arm capped with a rubber septum. The reactor vessel was then heated using a ThermoFisher Temperature bath to a steady temperature of 25°C. This allows for the evaporation of the acetaldehyde so that equilibrium can be reached between the solid catalyst and gas acetaldehyde. To monitor the reactivity of a given catalyst, 35 µL aliquots were taken every ten minutes from the reaction vessel and injected into a gas chromatography-mass spectrometer (Shimadzu, GC-MS QP500). The product monitored in these experiments was CO_2 and change in the concentration of acetaldehyde. To further test a sample visible light or ultraviolet light could be irradiated through the glass quartz top using an Oriel 1000W high pressure Hg lamp with corresponding colored glass filter. To better analyze the exact nature of the toluene/methanol mixed solvent systems 200 µL of acetaldehyde was used in place of 100 µL.

Figure 1-3 Shown above is the glass reaction vessel with the quart glass window top and the Oriel 1000W high pressure Hg lamp used to produce visible light.

1.8 Structure and Composition

PXRD patterns of manganese doped titania/silica show that the dominate phase of the titanium dioxide is anatase as confirmed by the PDF 3#87-1157. Shown in **Figure 1-4**, the amorphous silica is only seen at <= 2 theta and the anatase phase is well crystalline shown by the narrowing

of the diffraction patterns. Using the Scherer equation also shown in **Figure 1-4**, the average crystalline size is found to be 11nm. Although the dopant, manganese, is present at a 10 mol % ratio, no manganese diffraction patterns are observed. This is believed to be due to the substitution of Mn atoms in place of the Ti and Si atoms in the lattice structure. As the concentration of the Mn atoms is $1/10^{th}$ that of Ti and Si, the statistical difference caused by displacement would be minimal.

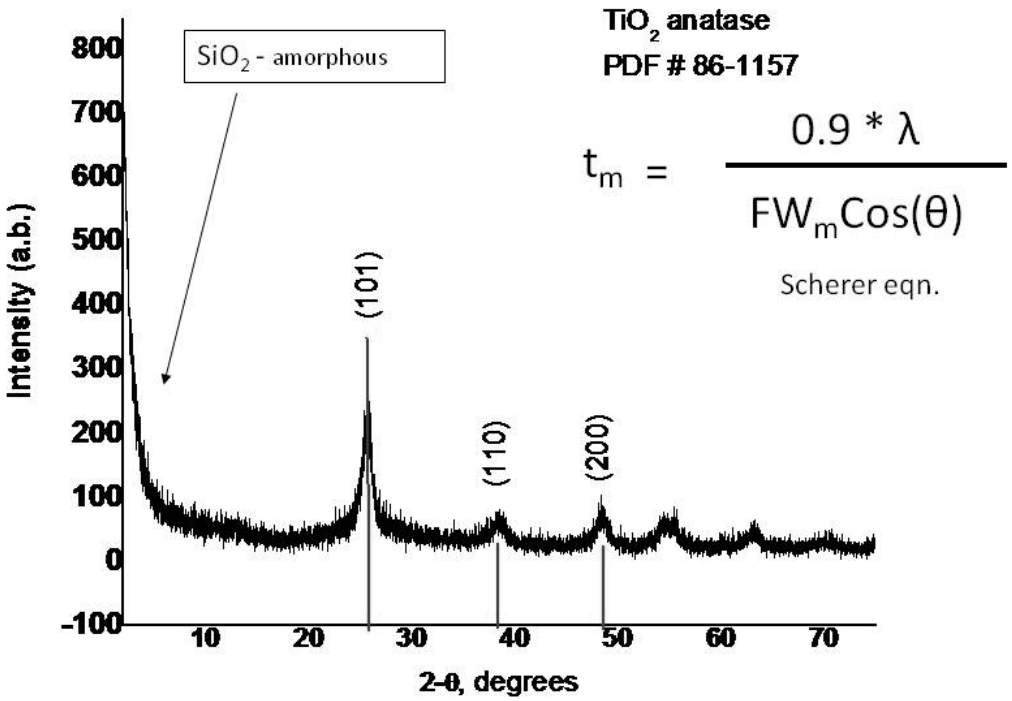

Figure 1-4 Shown above is the powder x-ray diffraction pattern of a manganese 10 mol % doped titania/silica catalyst. The crystalline pattern is distinctive of anatase phase TiO_2

Surface area and pore size distribution measurements were performed using BET and BJH models respectively for titania/silica doped aerogels. Surface area and pore size summary data can be found in **Table 1**. The surface areas of the prepared aerogels are significantly higher than commercially available titania, P25 Degussa which is 50 m^2/g.

The UV-Vis diffuse reflectance spectra shown in **Figure 1-5** shows that doping manganese into a titania/silica aerogel system results in a red shift as well as a significant increase in absorbance around λ= 550 nm. Also shown, doping silica into a titania system does not significantly affect the absorption properties of the catalyst.

Table 1-1 Shown below are the surface area, pore diameter and pore volume of sol-gel prepared aerogels consisting of titania/silica.[17]

10 Mol % metal-doped	Surface area (m^2/g)	Pore diameter (nm)	Pore volume (cm^3/g)
TiO_2/SiO_2	490	2.0	1.2
TiO_2/SiO_2 -Mn	390	8.3	1.3

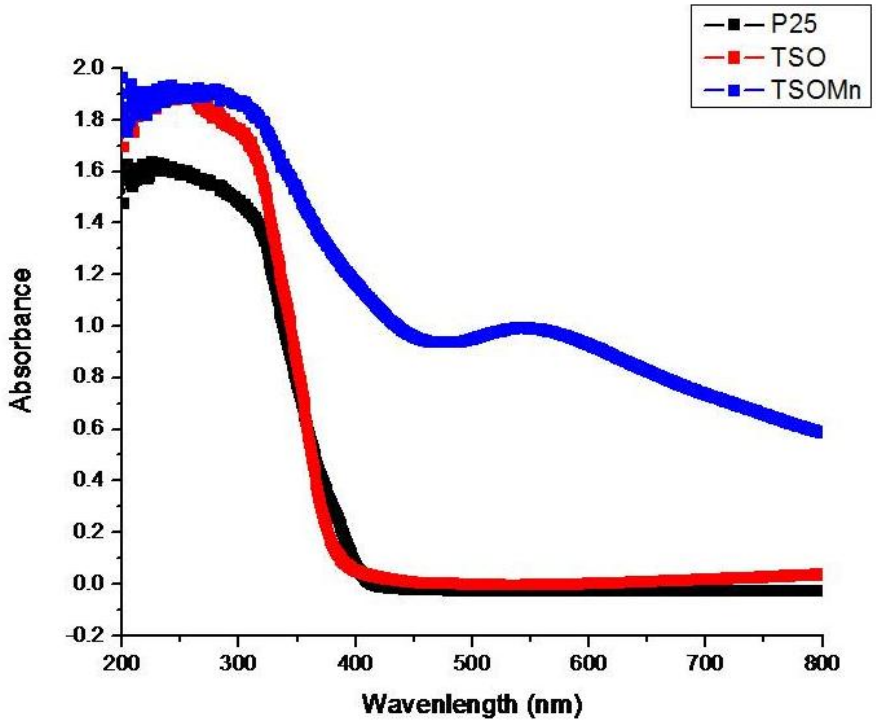

Figure 1-5 Shown above is the UV-Vis diffuse reflectance of commercially available P25 Degussa, sol-gel prepared Titania/Silica aerogel and sol-gel prepared Mn doped Titania/Silica. The addition of Si has little effect where as the addition of Mn causes a red shift.

1.9 Products of Photocatalysis of Acetaldehyde

Photocatalytic degradation experiments were carried out in a cylindrical glass reactor with a total volume of 305 mL and a quartz glass window allowing for direct light exposure. A circular glass stand was used to station the powdered aerogels above the liquid acetaldehyde with a magnetic stir bar under the stand. A typical experiment consisted of placing 100 mg of a given powdered aerogel in the stand and injecting 100 µL of liquid acetaldehyde (CH_3CHO) into a side arm capped with a rubber septum. The reactor vessel was then heated using a ThermoFisher Temperature bath to a steady temperature of 25°C. This allows for the evaporation of the acetaldehyde so that equilibrium could be reached between the solid catalyst and gaseous acetaldehyde. To monitor the reactivity of a given catalyst, 35 µL aliquots were taken every ten minutes from the reaction vessel and injected into a gas chromatography-mass spectrometer (Shimadzu, GC-MS QP500). The product monitored for these experiments was CO_2 and the concentration of the acetaldehyde over time. Visible light was irradiated through the glass quartz top using an Oriel 1000W high pressure Hg lamp with corresponding colored glass filter.

Photocatalytic degradation studies of acetaldehyde using 10 mol % manganese doped titania/silica show no degradation until visible light exposure has began as shown in **Figure 1-6**. The production of CO_2 also corresponds to the presence of visible light. The typical activity of this catalyst is the degradation of ~50% of the initial concentration of acetaldehyde while the production of CO_2 is only ~ 5% of the theoretical yield. A low yield of CO_2 is expected due to the large number of by products produced to yield CO_2 as explained below. Several other experiments using the 10 mol % manganese doped titania/silica catalyst will be summarized below. Additional experiments were performed testing the longevity of the catalyst. This was first observed upon an 8 hour experiment that resulted in a discoloration of the catalyst from a

dark purple (beginning) to a light purple/brownish (ending) powder. This suggested that the surface oxidation state was changing from Mn^{4+} to a proposed Mn^{2+}. A simple method exists for re-oxidizing these catalysts: calcine the used powdered aerogel at 500 °C for 2 hours at a rate of 5° C per minute. This changed the powder from a brown color corresponding to Mn^{2+} to its original dark purple color believed to be Mn^{4+}. Photo-activity was again achieved as well as the degradation of acetaldehyde and the production of CO_2 at the approximately the same rate as the first use of the catalyst.[17]

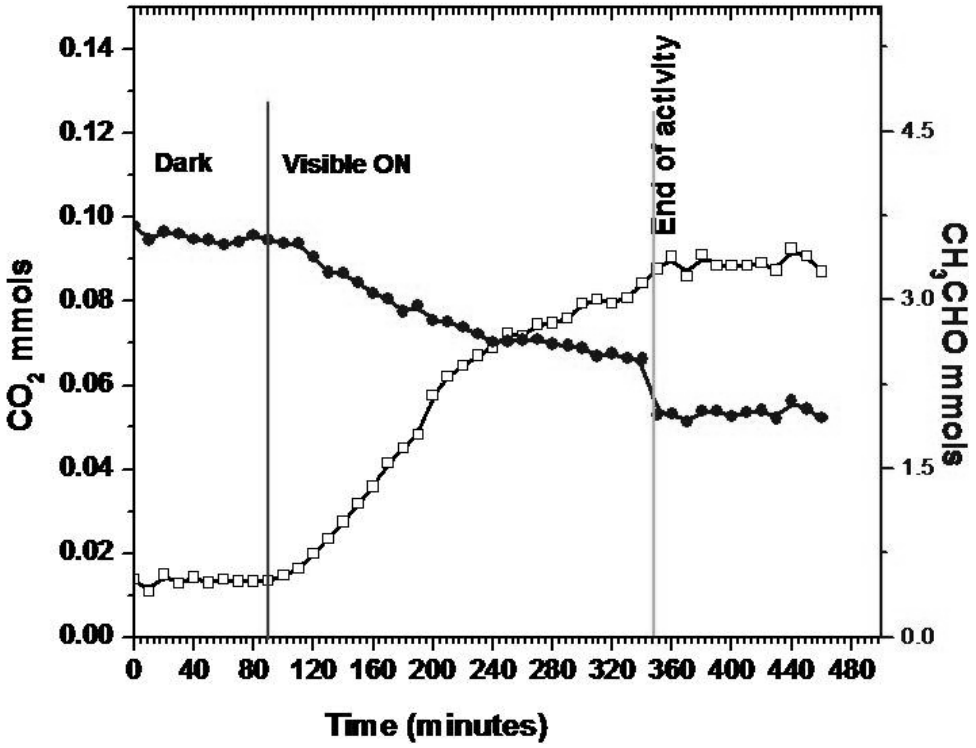

Figure 1-6 Shown above is a photo-activity study of 10 mol % manganese doped titania/silica. As shown the catalyst does not begin to adsorb or degrade acetaldehyde until visible light exposure begins. This also corresponds with the production of CO_2

The premise of developing a novel photocatalyst is utilizing the band gap of TiO_2. Since titania already has a band gap of 3.2 eV it is capable of absorbing ultraviolet light of λ=387 nm. This is a good starting point but the goal is to utilize these catalysts in an environmentally friendly

manner and more specifically in the indoor environment. It would therefore be counterproductive to use ultraviolet light in this environment. Visible light alternatively, represents ~ 46% of the total solar energy output of the sun each day and most office buildings contain windows or lights. It is therefore a practical assumption that visible light active catalysts would provide a great method for environmentally friendly remediation. A general representation of the activity of a photocatalyst is shown in **Figure 1-7**. The band gap is the difference between the valence band and conduction band which in TiO_2 is 3.2 eV or λ=387 nm. By introducing a dopant into titania we are in essence reducing the amount of energy required to promote an electron to the conduction band. In order to create an electron-hole pair, light of the right wavelength must strike the surface of the catalyst and promote an electron to the conduction band leaving a hole in the valence band.

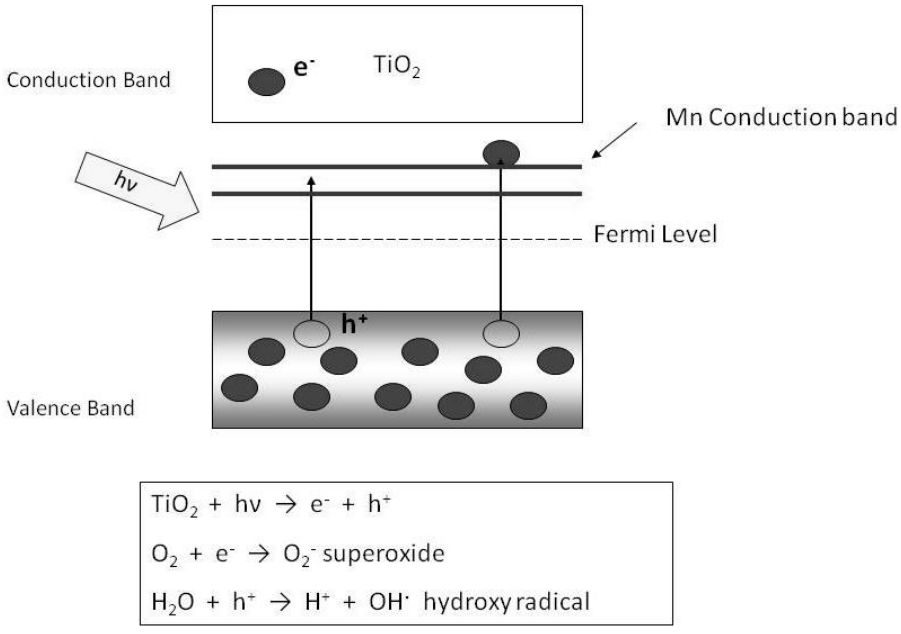

Figure 1-7 This representation of an electron-hole pair generation is the starting point for the mechanism of degradation of acetaldehyde. It is this the electron-hole pair that generate the O_2^- superoxide and OH· hydroxyl radical which lead to the eventual production of CO_2 from acetaldehyde.

The generation of the electron-hole pair is the first step leading to the creation of the O_2^- superoxide and OH· hydroxyl radical as shown in **Figure 1-7**. The generation of the O_2^- superoxide and OH· hydroxyl radical is important for the degradation of acetaldehyde as shown in the proposed mechanism **Figure 1-8**. When we talk about theoretical yield we assume that 100% of the starting products yield equal amounts (by mol) of products. In this case the turnover rate of acetaldehyde into CO_2 must first proceed through several steps or by products. This mechanism provides a justification of the loss of CO_2 production seen with these catalysts. These by-products were not monitored in the gas chromatography-mass spectrometer.

Believing this mechanism to be correct, experiments were designed to test for limiting reagents. An experiment using 100 µL of acetaldehyde and 100 mg of 10 mol % manganese doped titania/silica was run until the adsorption of acetaldehyde and production of CO_2 had come to a stop. At this point a known amount of O_2 was injected into the reactor. This resulted in the continued production of CO_2 and the degradation of more acetaldehyde.[17] This supports the proposed mechanism as O_2 is one of the side requirements for the production of CO_2 that would be limited in a closed container. To confirm changes in oxidation state of manganese ESR and XPS experiments were performed.

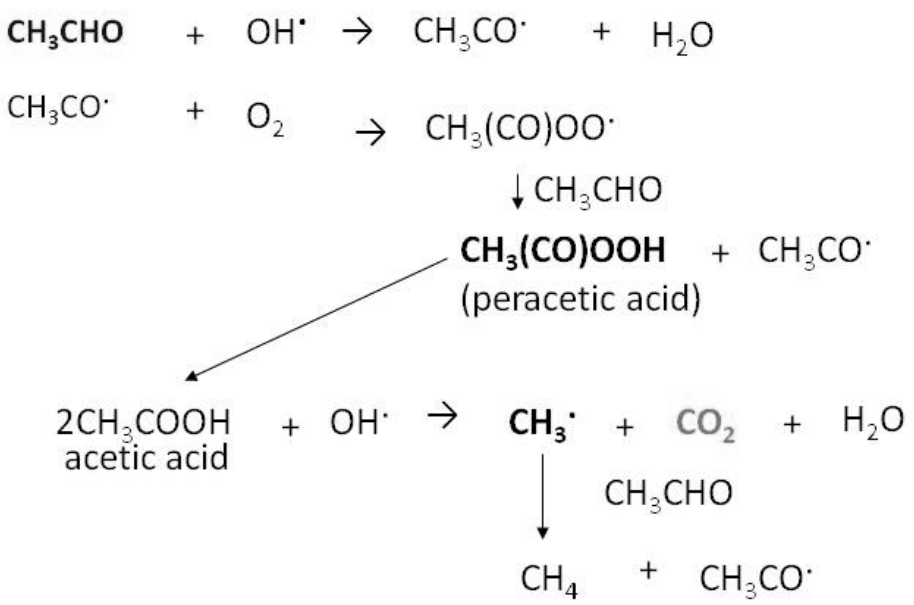

Figure 1-8 Proposed mechanism for the degradation of acetaldehyde leading to CO_2 production.[17]

1.10 Surface Oxidation

1.10.1 Electron Spin Resonance

Electron spin resonance studies were performed using a diluted manganese doped titania/silica sample (2 mol %), to analyze the oxidation state changes in the sample before and after samples were submitted. The resulting spectrum is shown in **Figure 1-9**. In the spectrum the before exposure to acetaldehyde, (smaller inner line) shows a sextet hyperfine splitting pattern which is characteristic of Mn^{4+}. The after exposure sample (larger overlayed line) shows a similar sextet splitting pattern but with the addition of peaks between the sextet. This splitting pattern was assigned Mn^{2+} since Mn^{3+} is ESR silent.[22,23] A 10 mol % manganese doped titania/silica sample was submitted for ESR analysis under the same conditions. The resulting spectra had strong overlapping lines caused by the increased loading of manganese which prevented the determination of the hyperfine lines.[17]

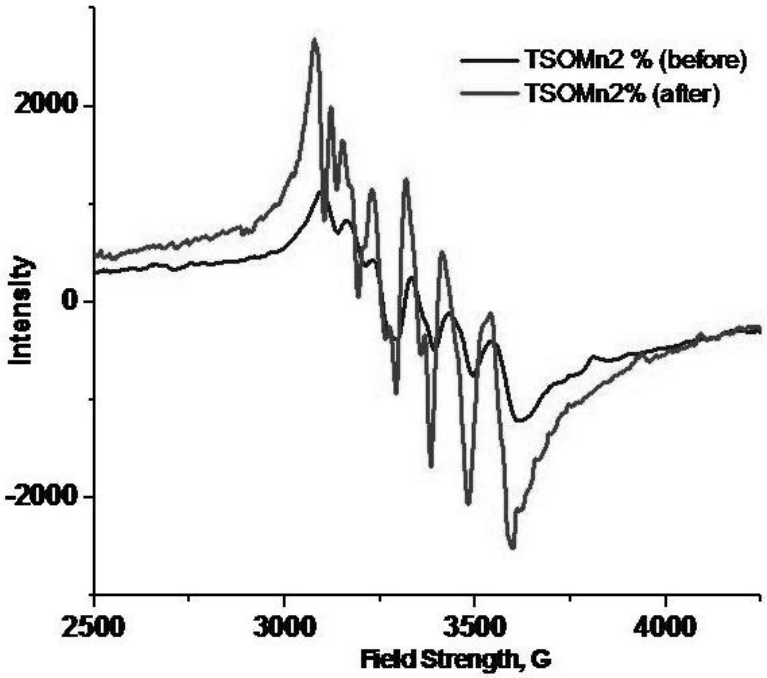

Figure 1-9 Electron Spin Resonance spectra showing the sextet pattern of Mn^{4+} before and the additional splitting of the sextet after caused by the Mn^{2+} state.[17]

1.10.2 X-ray Photo-electron Spectroscopy

X-ray photoelectron spectroscopy is a useful surface analysis that delves into the oxidation states of molecules present in the top 1-10 nm. Based on the results shown in **Figures 1-10, 1-11** and **1-12**, we are able to confirm earlier suspicions that the state of the 10 mol % manganese doped titania/silica system consists mainly of TiO_2-SiO_2-MnO_2. It was believed that the overall structure of the catalyst would consist of networked (-Ti-O-Si-O-) segmented in different forms ultimately resulting with a formula of ~ TiO_2-SiO_2-0.1MnO_2. Upon analysis of the before and after spectra it is obvious that there are no changes to any of the oxidation states shown in the XPS spectra. This further supports our hypothesis that the surface is being oxidized from Mn^{2+} after a reaction back to Mn^{4+} in the presence of light and O_2.

1.11 Benefits of Mixed Solvent Systems

Considerable amounts of research have been performed previously studying the effects of solvents on the overall gelation process using the sol-gel method.[10,17,22,23] These studies focused on the production of magnesium hydroxide from magnesium methoxide. A wide range of solvents were tested and carefully studied to find how they impacted the rate of gel formation and overall physical characteristics. These experiments studied the effects of solvent-to-methanol ratios of 0, 0.1, 0.4, 0.8, 1.6 and 1.96. Of particular interest to us were the results of the toluene/methanol solvent combination as it was found to result in the highest surface area gels. The gels synthesized using a toluene/methanol mixed solvent resulted in the formation of clear rigid gels. Using this method the surface area of magnesium hydroxide was increased from 348 m^2/g (methanol only) to 687 m^2/g (1.96 toluene/methanol solvent). The suggested mechanism is that the polarity of the solvent directly impacts the hydrolysis reaction rate. Non-polar solvents result in a faster hydrolysis and higher surface area gel where as the polar solvents result in a slower gelation and lower surface area. The slower hydrolysis is attributed to the possible formation of alkoxides.

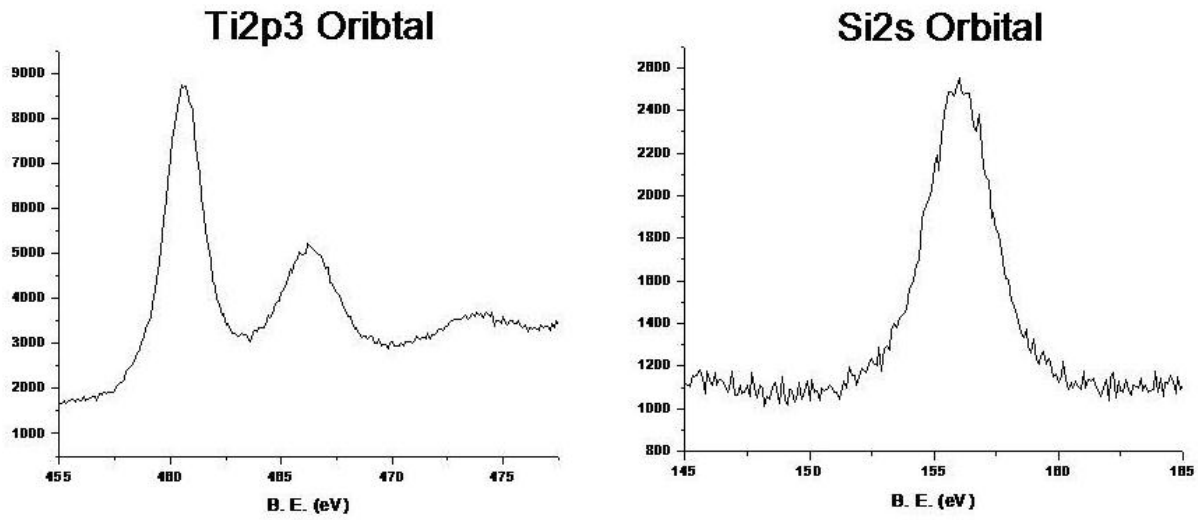

Figure 1-10 Shown above are XPS spectra of the Ti3p3 and Si2s orbitals. The Ti2p3 orbital shows a peak at ~460 eV which corresponds to the presence of TiO_2. The Si2s spectrum shows a peak at ~156 eV which represents SiO_2.

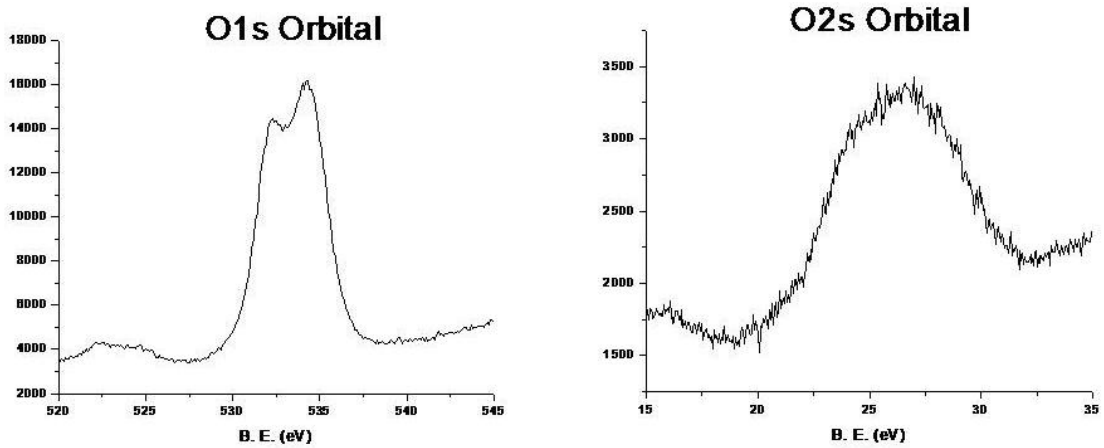

Figure 1-11 Shown above is the XPS spectra of the O1s and O2s orbital. The O1s spectrum shows a peak at ~532 eV which represents SiO_2 and the second peak ~532 eV H_2O. The O2s orbital diagram shows a peak at ~26 eV which corresponds to the presence of H_2O.

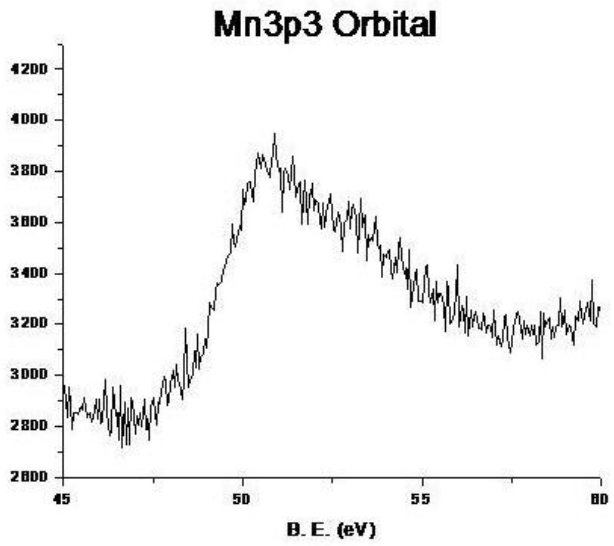

Figure 1-12 Shown above is the XPS spectra of the Mn3p3 orbital with a peak at ~51 eV. This corresponds to the presence of MnO_2.

1.12 Results of Mixed Toluene/Methanol Solvent

The first attempts at synthesizing manganese 10 mol % doped titania/silica systems using toluene/methanol as the solvent resulted in precipitation due to the addition of NH_4OH/H_2O too quickly. Although the base was added dropwise the reaction had to be carefully monitored for signs of early gelling or precipitation. If either of these was noticed, either by a slowing of the stirring or appearance of light purple particles in solution, the addition of NH_4OH/H_2O was stopped for one to two minutes and then again added drop wise. The resulting gels, a deep purple, formed within a matter of minutes and appeared to be very sturdy. The resulting gels were allowed to age for a period of 24 hrs and then subjected to supercritical drying via an autoclave at 265 °C. This process takes 4 hours and calcination follows immediately after this step at 500 °C for 2 hours. Calcining is a very important step for removing any organic contaminants that might still be present as well as increasing the crystalline phase of the anatase titania. **Figure 1-13** shows the physical appearance of the gel, as prepared aerogel and calcined aerogel. The BET data collected from sorption isotherms can be found in **Table 2**.

Figure 1-13 Shown above left to right is the wet gel, aerogel after supercritical drying and finally the calcined aerogel (finished product).

There are no distinct trends in surface area, pore diameter or pore volume except that they all remain relatively the same. This was an unexpected behavior as the reason for using a mixed solvent system, particularly toluene/methanol, was due to its ability to increase the surface area in silica systems dramatically. This could be due to the proximity of precipitation in the systems causing an unwanted plateau in surface area. There is still hope for these catalysts have relatively high surface areas >360 m^2/g.

Table 1-2 Shown below are the surface area, pore diameter and pore volume of synthesized mixed solvent systems (toluene/methanol) of 10 mol %manganese doped titania/silica.

Mn-TSO samples with varying solvents:	Surface area (m^2/g)	Pore diameter (nm)	Pore volume (cm^3/g)
Ethanol	390	2.0	1.2
Methanol	366	6.44	2.04
Toluene/Methanol 0.80 (vol)	364	1.93	1.84
Toluene/Methanol 1.60 (vol)	337	1.93	1.98
Toluene/Methanol 1.96 (vol)	370	1.72	1.57

A particularly interesting finding is in the shift caused in the UV-Vis diffuse reflectance spectra shown in **Figure 1-14**. The Mn-titania/Silica systems synthesized using methanol and a mixed toluene/methanol solvent show a slight red shift of 10-15 nm. All systems containing 10 mol % manganese doped onto titania/silica show a significant increase in absorption in the visible range as compared to the undoped system. These spectra show encouragement for active degradation of volatile organic compounds in the presence of visible light as they all posses a λ_{max}=550-560. To test for visible light activity 200 µL of acetaldehyde was placed in the 305 mL glass reactor vessels with 100 mg of powdered catalyst. The reason for using 200 µL of acetaldehyde was to rule out adsorption and clearly show if visible light was activating the catalyst.

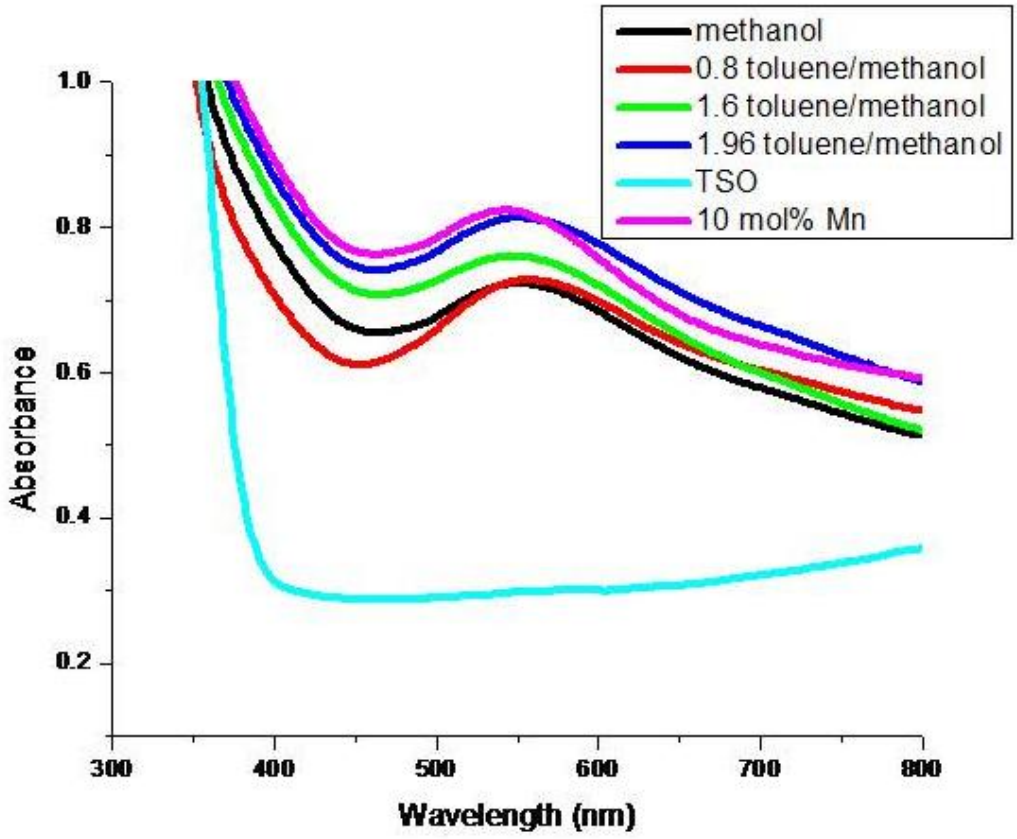

Figure 1-14 UV-Vis diffuse reflectance of all synthesized 10 mol % doped manganese titania/silica systems. The used of a mixed solvent system of toluene/methanol resulted in a ~10 nm red shift.

As seen in **Figure 1-15**, all four catalysts were able to remove up to ~94.0 % of the initial acetaldehyde concentration. The methanol only catalyst removed 94.4%, 08. Toluene/methanol removed 93.0%, 1.6 toluene/methanol removed 94% and the 1.96 toluene/methanol removed 93.4 % of the initial concentration. These calculations are based on the initial 200 µL being completely vaporized and reacted with the catalyst. The presence of visible light made no discernable difference in the degradation of acetaldehyde but an average removal of ~ 94 % of the total initial concentration of acetaldehyde was achieved across the board for all catalysts regardless of surface area. The production of CO_2 is shown in **Figure 1-16**. The overall production of CO_2 was rather low for all catalysts. The methanol only catalyst yielded only 2.8%, 0.8 toluene/methanol 2.2%, 1.6 toluene/methanol 3.0% and 1.96 toluene/methanol yielded 2.4% of the theoretical yield of 7.12 mmol. Moreover the exposure to visible light had no impact on the production of CO_2 for any of the catalysts.

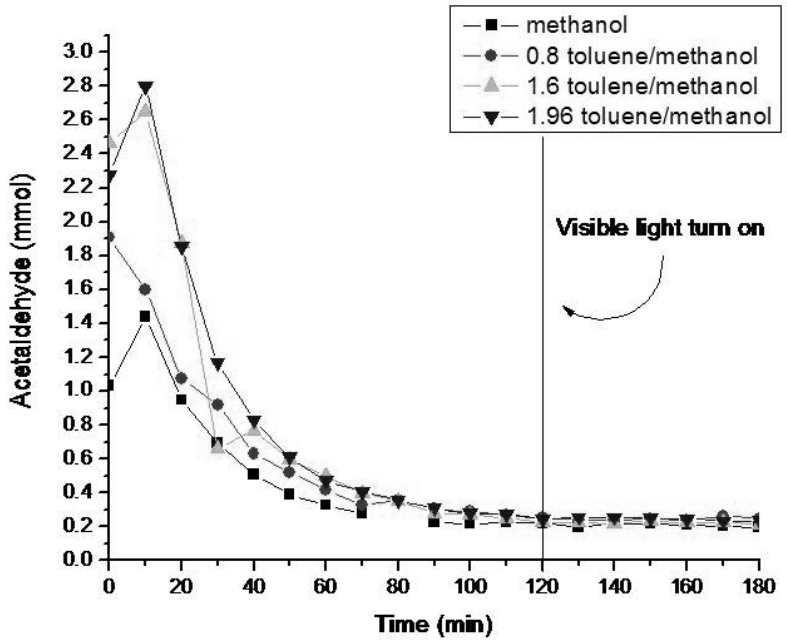

Figure 1-15 Shown here are the degradation studies of the mixed toluene/methanol solvent systems. These systems are derived from the 10 mol % manganese doped titania/silica catalysts previously studied. These catalysts show no activity towards visible light but show an enhanced ability to degrade acetaldehyde.

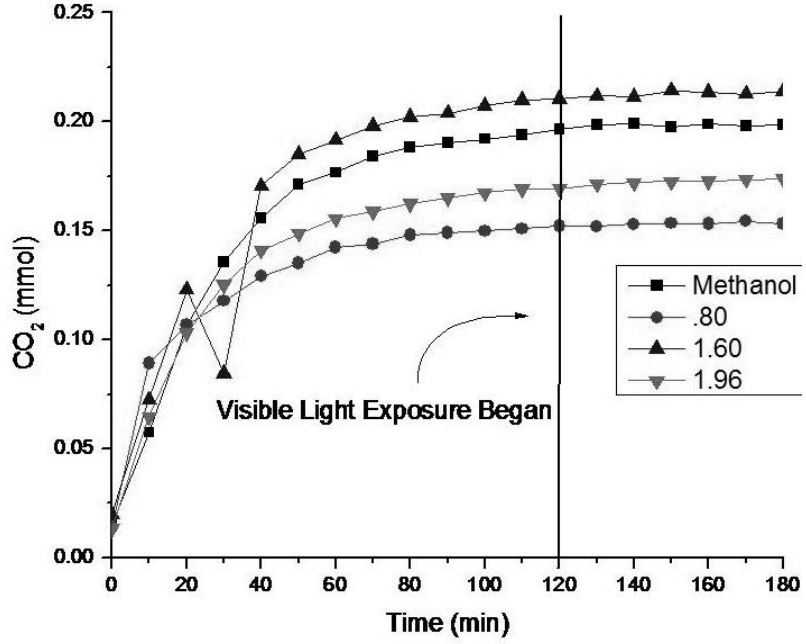

Figure 1-16 The production of CO_2 via the mixed solvent system catalysts is limited and not affected by the exposure to visible light as shown.

1.13 Conclusions

Manganese doped titania/silica systems show promising uses as photocatalysts and as sorbents. The use of a single solvent system results in a good photocatalyst capable of degrading acetaldehyde and producing CO_2 in the presence of visible light. This catalyst works so effectively because of the surface oxidation chemistry that allows for the reactivation of the catalyst via low temperature reoxidation. These reactions can be further enhanced by the introduction of additional volumes of O_2 to the system preventing it from being a limiting reagent in the production of CO_2. This catalyst is also able to re-oxidize its surface to Mn^{4+} in the presence of light and O_2 as shown through the combination of ESR and XPS data. Mixed solvent systems using toluene/methanol resulted in the creation of a new series of good sorbent materials capable of producing moderate quantities of CO_2 as compared to other catalysts of similar configurations but are capable of absorbing up to 95% of the initial concentrations of the pollutant.

1.14 References

(1) Kesselmeier, J.; Staudt, M. Biogenic volatile organic compounds (VOC): an overview on emission, physiology and ecology. *J. Atmos. Chem.* **1999**, *33*, 23-88.

(2) Schauer, J. J.; Kleeman, M. J.; Cass, G. R.; Simoneit, B. R. T. Measurement of Emissions from Air Pollution Sources. 5. C1-C32 Organic Compounds from Gasoline-Powered Motor Vehicles. *Environ. Sci. Technol.* **2002**, *36*, 1169-1180.

(3) Schauer, J. J.; Kleeman, M. J.; Cass, G. R.; Simoneit, B. R. T. Measurement of Emissions from Air Pollution Sources. 3. C1-C29 Organic Compounds from Fireplace Combustion of Wood. *Environ. Sci. Technol.* **2001**, *35*, 1716-1728.

(4) Schauer, J. J.; Kleeman, M. J.; Cass, G. R.; Simoneit, B. R. T. Measurement of Emissions from Air Pollution Sources. 1. C1 through C29 Organic Compounds from Meat Charbroiling. *Environ. Sci. Technol.* **1999**, *33*, 1566-1577.

(5) Schauer, J. J.; Kleeman, M. J.; Cass, G. R.; Simoneit Bernd, R. T. Measurement of emissions from air pollution sources. 4. C1-C27 organic compounds from cooking with seed oils. *Environ Sci Technol* **2002**, *36*, 567-575.

(6) An Introduction to Indoor Air Quality (IAQ). *http://www.epa.gov/iaq/voc.html* (accessed 08/03, 2011).

(7) Zhao, X. S.; Ma, Q.; Lu, G. Q. VOC Removal: Comparison of MCM-41 with Hydrophobic Zeolites and Activated Carbon. *Energy Fuels* **1998**, *12*, 1051-1054.

(8) Heiderscheidt, J. L.; Crimi, M.; Siegrist, R. L.; Singletary, M. A. Optimization of full-scale permanganate ISCO system operation: laboratory and numerical studies. *Ground Water Monit. Rem.* **2008**, *28*, 72-84.

(9) Fujishima, A.; Honda, K. Electrochemical photolysis of water at a semiconductor electrode. *Nature (London)* **1972**, *238*, 37-38.

(10) Demydov, D.; Klabunde, K. J. Characterization of mixed metal oxides (SrTiO3 and BaTiO3) synthesized by a modified aerogel procedure. *J. Non-Cryst. Solids* **2004**, *350*, 165-172.

(11) Hamal, D. B.; Klabunde, K. J. Synthesis, characterization, and visible light activity of new nanoparticle photocatalysts based on silver, carbon, and sulfur-doped TiO2. *J. Colloid Interface Sci.* **2007**, *311*, 514-522.

(12) Yang, X.; Cao, C.; Erickson, L.; Hohn, K.; Maghirang, R.; Klabunde, K. Synthesis of visible-light-active TiO2-based photocatalysts by carbon and nitrogen doping. *J. Catal.* **2008**, *260*, 128-133.

(13) Yang, X.; Cao, C.; Hohn, K.; Erickson, L.; Maghirang, R.; Hamal, D.; Klabunde, K. Highly visible-light active C-doped and V-doped TiO2 for degradation of acetaldehyde. *J. Catal.* **2007**, *252*, 296-302.

(14) Kapoor, P. N.; Heroux, D.; Mulukutla, R. S.; Zaikovskii, V.; Klabunde, K. J. High surface area homogeneous nanocrystalline bimetallic oxides obtained by hydrolysis of bimetallic μ-oxo alkoxides. *J. Mater. Chem.* **2003**, *13*, 410-414.

(15) Kapoor, P. N.; Uma, S.; Rodriguez, S.; Klabunde, K. J. Aerogel processing of MTi2O5 (M=Mg, Mn, Fe, Co, Zn, Sn) compositions using single source precursors: synthesis, characterization and photocatalytic behavior. *J. Mol. Catal. A: Chem.* **2005**, *229*, 145-150.

(16) Wang, J.; Uma, S.; Klabunde, K. J. Visible light photocatalysis in transition metal incorporated titania-silica aerogels. *Appl. Catal. , B* **2004**, *48*, 151-154.

(17) Kalebaila, K. K.; Klabunde, K. J. An inorganic oxide TiO2-SiO2-Mn aerogel for visible-light induced air purification. *ACS Symp. Ser.* **2010**, *1045*, 207-223.

(18) Hench, L. L.; West, J. K. The sol-gel process. *Chem. Rev.* **1990**, *90*, 33-72.

(19) Cushing, B. L.; Kolesnichenko, V. L.; O'Connor, C. J. Recent Advances in the Liquid-Phase Syntheses of Inorganic Nanoparticles. *Chem. Rev. (Washington, DC, U. S.)* **2004**, *104*, 3893-3946.

(20) Velu, S.; Shah, N.; Jyothi, T. M.; Sivasanker, S. Effect of manganese substitution on the physicochemical properties and catalytic toluene oxidation activities of Mg-Al layered double hydroxides. *Microporous Mesoporous Mater.* **1999**, *33*, 61-75.

(21) Keeble, D. J.; Li, Z.; Poindexter, E. H. Electron paramagnetic resonance of Mn4+ in PbTiO3. *J. Phys. : Condens. Matter* **1995**, *7*, 6327-6333.

(22) Ranjit, K. T.; Martyanov, I.; Demydov, D.; Uma, S.; Rodrigues, S.; Klabunde, K. J. A review of the chemical manipulation of nanomaterials using solvents: Gelation dependent structures. *J. Sol-Gel Sci. Technol.* **2006**, *40*, 335-339.

(23) Carnes, C. L.; Kapoor, P. N.; Klabunde, K. J.; Bonevich, J. Synthesis, Characterization, and Adsorption Studies of Nanocrystalline Aluminum Oxide and a Bimetallic Nanocrystalline Aluminum Oxide/Magnesium Oxide. *Chem. Mater.* **2002**, *14*, 2922-2929.

Chapter 2 - Synthesis of Cobalt Doped Titania/Silica Aerogels Exhibiting Dark Activity for Degradation of Acetaldehyde

2.1 Introduction

The primary goal of our research was to develop novel materials for use in remediation of the indoor air environment. Air pollution indoors arises from the release of gases and particles into the air. This problem is further enhanced by poor ventilation due to the lack of air coming into the home to dilute these pollutants as well as the lack of diffusion of air out of the home removing the pollutants. The concentration of certain pollutants can be increased due to high temperatures and humidity levels. Some common sources of indoor air pollution[1.2.3.4] are: combustion of oil, gas, kerosene, coal, wood and tobacco products, asbestos, household cleaning and personal care products, pesticides and outdoor air pollution. These sources can cause a wide range of adverse health effects (short term) such as irritation of the eyes, nose, and throat, dizziness, fatigue or headaches, which are often treatable. They can also be long-term effects such as respiratory disease, heart disease, cancer and other effects can be severely debilitating or even fatal. This information provides an overview of all air pollution which can occur in the indoor environment. For the purpose of environmental remediation research, the entire spectrum of pollution is too overwhelming. We therefore narrowed the scope to pollutants of a nature easy to work with in the lab. For this reason we choose volatile organic compounds, VOCs.

According to the EPA volatile organic compounds are gases which evolve from certain solids or liquids. These gases can have many varying adverse health effects such as headache, nausea, loss of coordination, as well as damage to the liver, kidney, and central nervous system.[5] These gases evolve from many common materials used inside such as asbestos, household cleaning products and personal care products. Certain studies have shown that the concentration level of

several organics that can be found inside homes are two to five times higher than outdoors.[5] In recent years the affects of these compounds on our health has been drawing attention. As a result measures have been taken to reduce the emission of these gases but this is generally regulation is limited to the outdoor environment. It is our responsibility to help change the perception of the general population as the majority of workers spend eight to ten hours a day working from an office or enclosed environment.

2.2 Previous Methods of Remediation

When beginning a project it is important to understand what methods have been used previously, which worked and which did not. One of the simplest methods for removing gases from an environment is to use adsorption. High surface area materials, such as activated carbon[6], often work well at adsorbing gases. The flaw in this method is that the material draws the gas out of the air and concentrates the pollutant on the surface of the material rather than destroying it. In many ways this creates a bigger problem by concentrating the pollutant. Another method is chemical oxidation of the pollutant degrading the pollutant into other products. This method requires often toxic materials such as permanganates[7] and persulfates which can be fairly expensive and typically are not very robust. Our aim is to establish novel methods for air remediation that are both inexpensive and destructive. A method for achieving this goal would be the use of photocatalysis via titania.[8]

2.3 Promising Catalyst: Titania

Titania based catalysts have become increasingly important due to their activity at room temperature, inert, nontoxic and the nature of their band gaps. It is for these reasons that titania was chosen to be used as the base for developing novel catalysts for environmental remediation. Titania (TiO2) has a band gap between 3.0-3.2 eV depending on the crystalline phase. The

catalysts synthesized in this paper utilize anatase phase titania, band gap 3.2 eV, because of its known photo-activity in the ultraviolet range (387.5 nm) and low heat treatment.9,10 Although the ability to utilize ultraviolet light active is a start, UV light only accounts for ~ 5% of the solar energy and is dangerous to be exposed to constantly in an enclosed space. Therefore the goal is to use dopants that shift the band gap into the visible light absorbing region. This has been achieved using many different dopants: carbon,10,11 sulfur10, nitrogen12 and more recently transition metals.5,7,9 In attempts to improve the activity of the catalyst, it has been found that increasing the surface area can lead to an increase in the absorption and degradation of pollutants.10,13,14.15 To increase the surface area titania is mixed with silica which allows for an increase in the surface area without excessive changes in the overall activity of the catalyst and in some cases even enhances the activity.

2.4 Modified Sol-Gel Method

The sol-gel method generally refers to the hydrolysis and condensation of alkoxide precursor. One of the most common alkoxide precursors is $Si(OEt)_4$, tetraethyl orthosilicate. One of the first recorded examples of sol-gel chemistry is by Ebelmen in the 1840's.[16] The sol-gel method is of particular interest because of its ability to produce a high surface area material that is homogenous in nature. The sol-gel process[17,18] can be described by a series of five steps. The first step is the formation of the sol. The second step is gelation, which occurs as a result of the formation of an oxide or more commonly alcohol bridged network. Step three consists of aging of the gel known as syneresis during which polycondensation reactions continue until a lack of precursors. The fourth step is the drying of the gel which can occur in two very different ways. The first method of drying gel is simply to allow the gel to air dry or under mild heating which results in the formation of a xerogel characteristically having smaller pores than the second

method. The second method is to place the gel in an autoclave and heat the gel above its super critical point removing the solvent from the pores without causing the collapse of the pores. This method produces an aerogel. The fifth step is densification of the resulting powdered gel via heat treatment at 500 °C.

The first attempts at creating a gel using this method led to a dark green liquid which was allowed to gel over the period of several days. This led to gelation at the bottom of the flask but a large amount of solvent remained. In an attempt to have a more homogeneous gelation process, the addition of NH_4OH and water was added instantaneously, rather than drop wise. The hope was to achieve a quick gel without the formation of a precipitate.

To test the activity of a catalyst, 100 µL of acetaldehyde was placed in a 305 mL cylindrical reaction vessel and mixed with 100 mg of powdered aerogel. The concentration of acetaldehyde and CO_2 was monitored via gas-chromatography mass spectrometry. This equates to about 1.78 mmol of acetaldehyde which theoretically should react in the following manner:

$$2CH_3CHO + 5O_2 \rightarrow 4CO_2 + 4H_2O$$

As shown above, for every two moles of acetaldehyde 4 moles of CO_2 is produced. GC-MS monitoring began immediately after injecting the acetaldehyde into the reactor vessel. This allowed for the observation of the vaporization and physical adsorption of the acetaldehyde as it moved from liquid to the vapor phase.

2.5 Synthesis of Titania/Silica Gels

Titania-silica (TiO_2-SiO_2) gel composites were synthesized by combining 8 mL TEOS in 62 mL of ethanol and 0, 0.21, 2, and 4 mL of ethyl acetoacetate for respective ratios no chelate, 1:10, 1:1 and 2:1. 10.5 mL of $Ti(O^iPr)_4$ was then added to this solution slowly. The ratios used are moles of ethyl acetoacetate (chelate) to moles Ti/Si. This solution was stirred for ca. ten minutes

while solution two was prepared. Solution two consists of dissolving 1.28 g of cobalt (III) acetyl acetonate in 14 mL of ethanol and stirring for 10 minutes. After solutions one and two have both had time to dissolve solution two is added to solution one and rinsed with a small amount of ethanol to remove any residual cobalt (III) acetyl acetonate. This solution is then allowed another 10 minutes of stirring while a solution of NH_4OH (1.5 mL) and H_2O (10 mL) is mixed. After solution three has stirred for 10 minutes the NH_4OH/H_2O is injected using a syringe in one continuous and quick shot. The resulting solution was allowed ca. 24 hours to age. The resulting gels were placed in an autoclave where they were heated under N_2 pressure to 265° C. This process takes 4 hours to complete. Immediately following autoclave treatment the resulting powder is ground using a mortar and pestle and calcined using a furnace to 500 °C for 2 hours at a rate of 5 °C per minute.

2.6 Characteristics

Powder X-ray diffraction (PXRD) was used to identify the crystallite phase present in titania/silica doped aerogels. PXRD data was obtained using a Scintag XDS 200D8 diffractometer equipped with a copper anode with a Kα radiation wavelength of 0.15406 nm from 2-75° (2θ). Samples were prepared for PXRD study by spreading a small amount of powdered aerogel onto a quartz background plate.

The Brunauer-Emmett-Teller (BET) surface area and the Barret-Joyner-Halenda (BJH) pore size distribution of the doped aerogels were obtained from nitrogen adsorption/desorption isotherms using a 30 sec equilibrium interval on a NOVA 1000 series Quantachrome Instrument acquired at 77 K. The samples were degassed to remove any adsorbed molecules at 200 °C for about 2 hours prior to analysis.

Solid state UV-Vis absorption was studied using a CARY 500 UV/VIS/NIR spectrophotometer equipped with an integrating sphere between 200-800 nm wavelength. The instrument was calibrated using a light reflecting powder as a reference (1 micron polytetrafluoroethylene).

2.7 Photocatalysis

Photocatalytic degradation experiments were carried out in a cylindrical glass reactor consisting of a total volume of 305 mL and a quartz glass window. A circular glass stand was used to station the powdered aerogels away from the liquid acetaldehyde with a magnetic stir bar under the stand. A typical experiment consisted of placing 100 mg of a given powdered aerogel in the stand and injecting 100 µL of liquid acetaldehyde (CH_3CHO) into a side arm capped with a rubber septum. The reactor vessel was then heated using a ThermoFisher Temperature bath to a steady temperature of 25°C. This allows for the evaporation of the acetaldehyde so that equilibrium could be reached between the solid catalyst and gaseous acetaldehyde. To monitor the reactivity of a given catalyst, 35 µL aliquots were taken every ten minutes from the reaction vessel and injected into a gas chromatography-mass spectrometer (Shimadzu, GC-MS QP500). The product monitored was CO_2 and the concentration of the acetaldehyde over time. To further test a sample, visible light or ultraviolet light could be irradiated through the glass quartz top using an Oriel 1000W high pressure Hg lamp with corresponding colored glass filter.

2.8 Structure and Composition

PXRD patterns of cobalt doped titania/silica are amorphous in nature but aerogel material shows a greater extent of crystalline phase than the xerogel. Due to the noise of the spectra caused by the amorphous nature, it is not possible to determine crystalline size using the Scherer equation. Based on the spectra of the cobalt doped titania/silica aerogel, the crystalline phase forming is characteristic of the diffraction patterns of anatase titanium dioxide except that it is impossible to

determine peaks in the 40° and 50° regions. The surface areas and pore sizes obtained from using BET and BJH models can be found in **Table 2-1**. These surface areas are considerably higher than a commercially available titania, P25 Degussa (50 $m^2/_g$) but are less than the undoped titania/silica system (490 $m^2/_g$) prepared using the same method.

Table 2-1 Shown below are the surface area, pore diameter and pore volume of sol-gel prepared aerogels 10 mol % cobalt doped titania/silica.. These aerogels were synthesized using various chelate concentrations to improve gelation and surface area.

	Surface area (m^2/g)	Pore diameter (nm)	Pore volume (cm^3/g)
No Chelate	199	3.79	0.53
1:10 Chelate to TSO	210	4.85	0.82
1:1 Chelate to TSO	279	12	0.87
2:1 Chelate to TSO	295	7.67	0.96

The first attempt at synthesizing a 10 mol % cobalt doped TiO_2/SiO_2 gel resulted in a slow and incomplete gelation. As shown in **Figure 2-1**, the bottom of the erlenmeyer flask contains what appears to be a gel and a substantial amount of the solvent. The solution above the gel is still a dark green hinting at the presences of cobalt ions. Unsure if the bottom material was a gel or precipitation; the two phases were separated and treated differently. The liquid phase was rotovaped and calcined to produce a xerogel and the solid phase was autoclaved to produce an aerogel. The crystalline structure of these materials was studied via PXRD as shown in **Figure 2-2**. The resulting x-ray diffraction patterns show an amorphous material with no distinctive patterns. The aerogel material shows a more crystalline but not definitive pattern. These two materials were subjected to UV-Vis diffuse reflectance to observe any absorption in the visible range. As shown in **Figure 2-3**, both materials exhibit absorption in the visible range with the 10 mol % cobalt doped TiO_2/SiO_2 material showing a higher absorption than a TiO_2/SiO_2 aerogel

prepared in a similar fashion. Spectra collected of the varying chelate synthesized materials can be found in **Figure 2-4**.

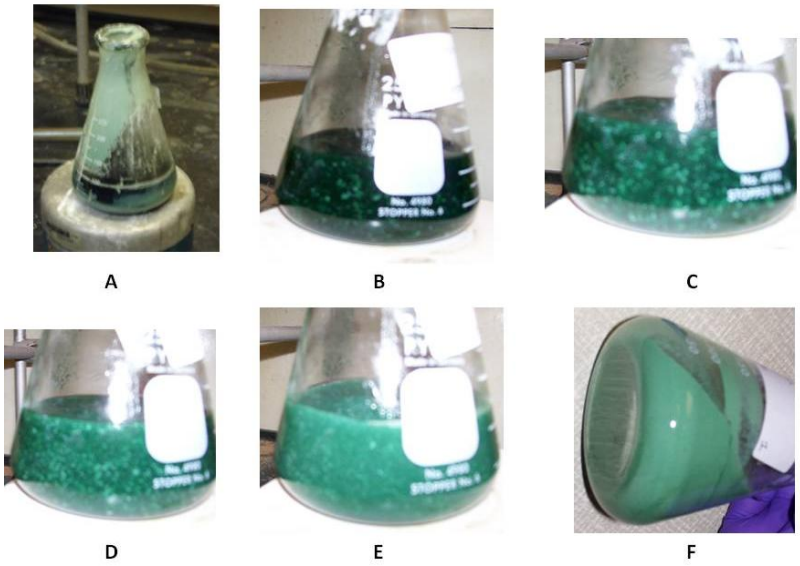

Figure 2-1 A) Initial experiment, which results in the formation of a gel but left a large amount of solvent in the liquid phase above. The follow images B-F show a typical reaction of the Co doped titania/silica system. B) The dissolved cobalt (III) acetyl acetonate results in a dark green solution. Upon the addition of the NH_4OH/H_2O light green particles begin to form and slowly build up the gel as seen in B-F.

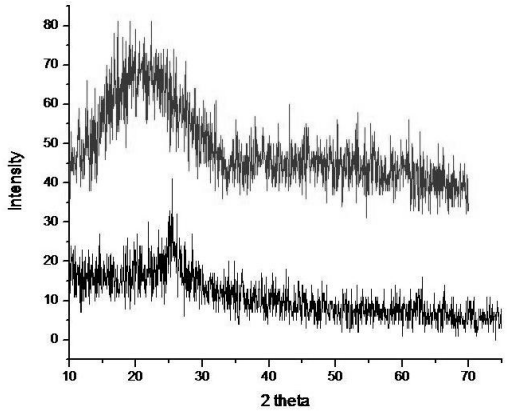

Figure 2-2 Shown above is the PXRD diffraction pattern of Co doped titania/silica prepared as an xerogel (top) which has no distinctive crystalline patterns. The bottom diffraction pattern shown is of the aerogel counterpart which resembles that of anatase phase TiO_2

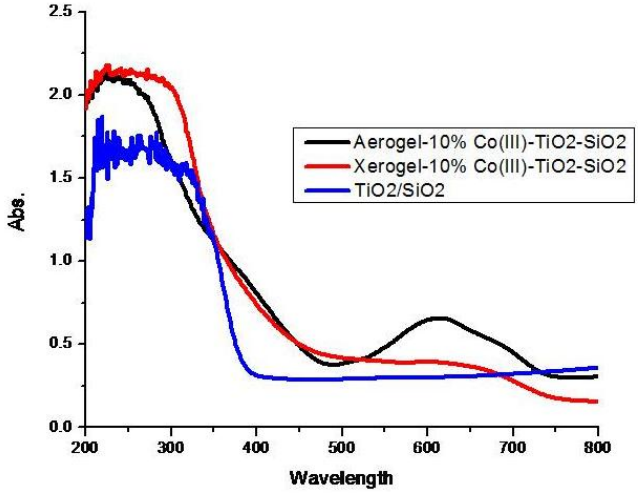

Figure 2-3 Shown above is the UV-Vis diffuse reflectance spectra of the resulting initial Co doped titania/silica systems. The addition of Co to the titania/silica system results in a slight red shifted peak formation in the xerogel and a more pronounced peak with the aerogel method.

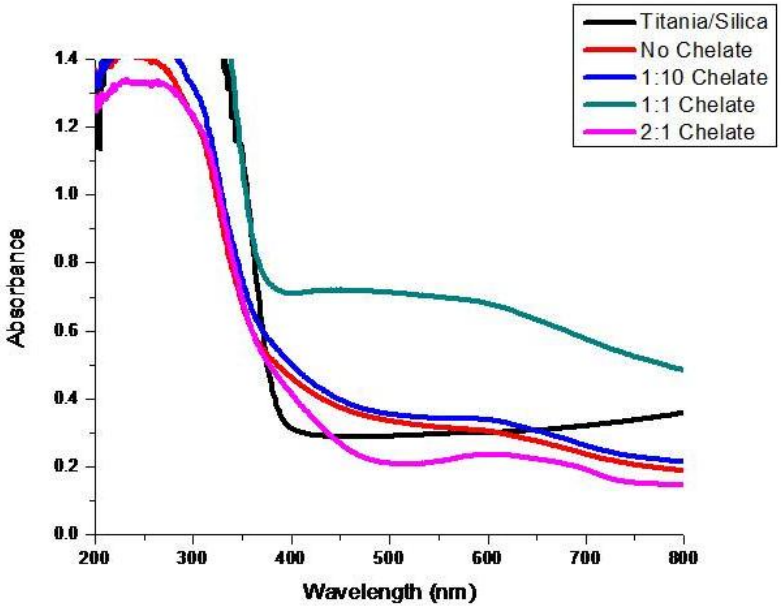

Figure 2-4 The variation of ethyl acetoacetate concentrations shown above result in unique changes in the absorbance. These changes could be caused by changes in presence of titanium, silicon or cobalt oxides resulting in a variation in delocalization of the d electrons.

The changes in the absorption of the cobalt doped TiO_2/SiO_2 aerogels can be explained by the changes made using varying amounts of chelating agent. These materials are mixed metal oxides doped with cobalt metal meaning that the change in absorption of the material could be caused by varying the delocalization of the d electrons. In other words, the change in the of TiO_2, SiO_2 or MnO_2

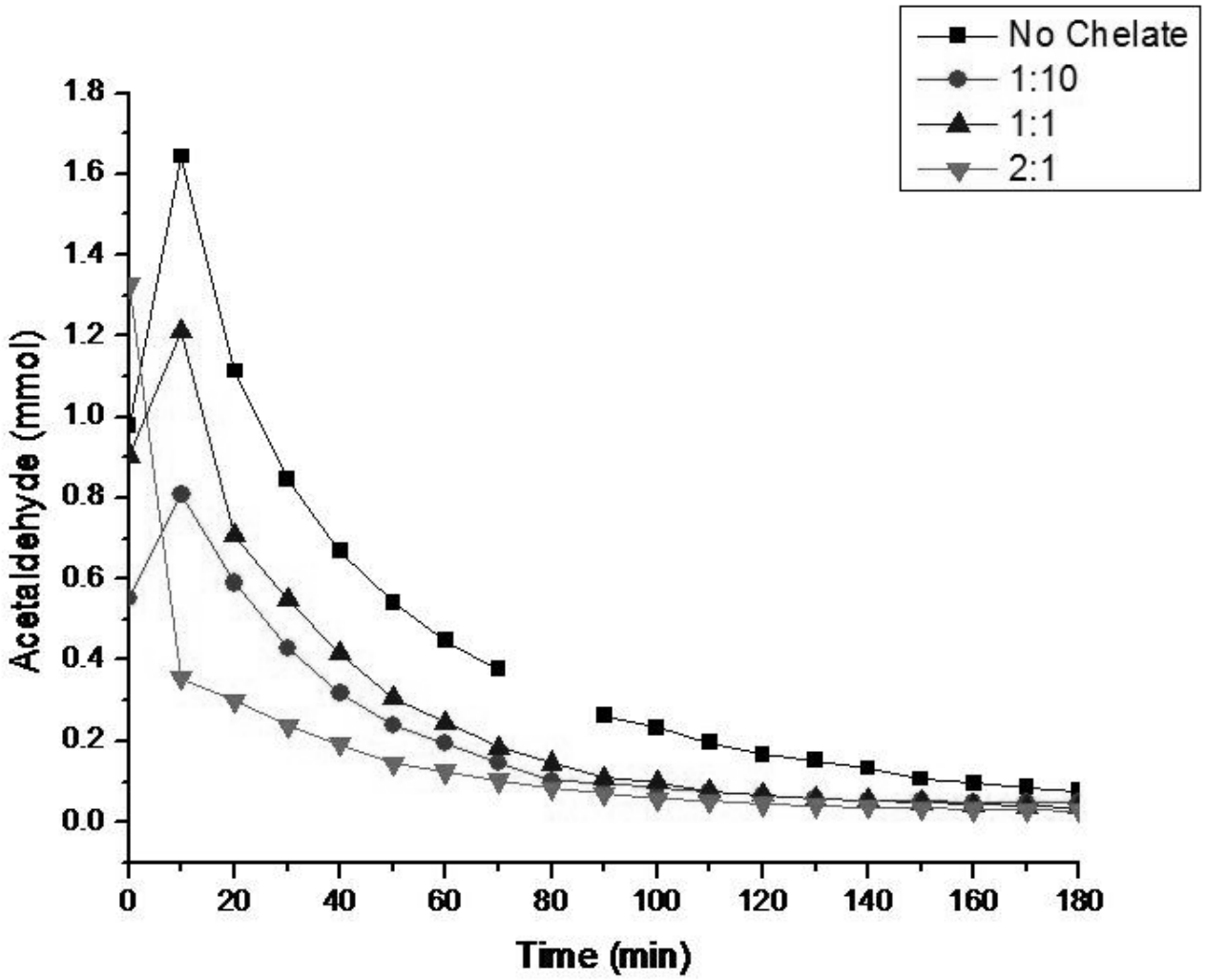

Figure 2-5 The degradation studies shown above were performed using 100 µL of acetaldehyde reacted with 100 mg of powdered cobalt doped titania/silica aerogels synthesized using various chelate concentrations. All four synthesized aerogels result in the removal of >95% of the initial acetaldehyde. Visible light exposure began at 120 minutes but resulted in no change of the removal of acetaldehyde.

2.9 Results

Based on the initial experiment which resulted in the formation of some gel but left a vast amount of solvent, it was determined that the gelation of a cobalt doped mixed metal oxide would have to be monitored. As a result, the variation of the chelating agent, ethyl acetoacetate, was studied at 0, 1:10, 1:1 and 2:1 (chelate to Ti/Si concentration based on mole %). The resulting surface areas, shown previously in **Table 2-1,** show a distinctive trend. The surface area increases from 199 m^2/g (no chelate) up to 295 m^2/g (2:1 chelate), in other words as the concentration of chelate is increased, the surface area increases. There is also an increase in the pore diameter and pore volume. A variation in the formation of titanium, silicon and cobalt oxide bonds, which are disrupted by the chelate, could lead to an increase in the surface area.

These four aerogels exhibit very strange behavior in the presence of acetaldehyde. In most cases the ten minute mark showed the largest concentration of acetaldehyde as seen in **Figure 2-5**. Within a period of 180 minutes all four aerogels have degraded as much acetaldehyde as possible and CO_2 production has leveled off. All four aerogels show a removal of over 95% of the initial 1.78 mmol of acetaldehyde. The exact removal percentages are as follow: 95.7%, 97.3%, 97.9% and 98.4% for no chelate, 1:10, 1:1 and 2:1 chelate respectively. The CO_2 production on the other hand has no distinct trend at first glance except that all catalysts produced less than 15% of the theoretical 3.56 mmol possible. For a 100 µL experiment there is a cap of ~ 0.5 mmol of CO_2 and for 200 µL about 1.0 mmol as illustrated in **Figures 2-6 and 2-7.** These percentages of CO_2 production could be a result of a complicated mechanism with many byproducts resulting in a low yield of CO_2 as with the manganese doped TiO_2/SiO_2 system.

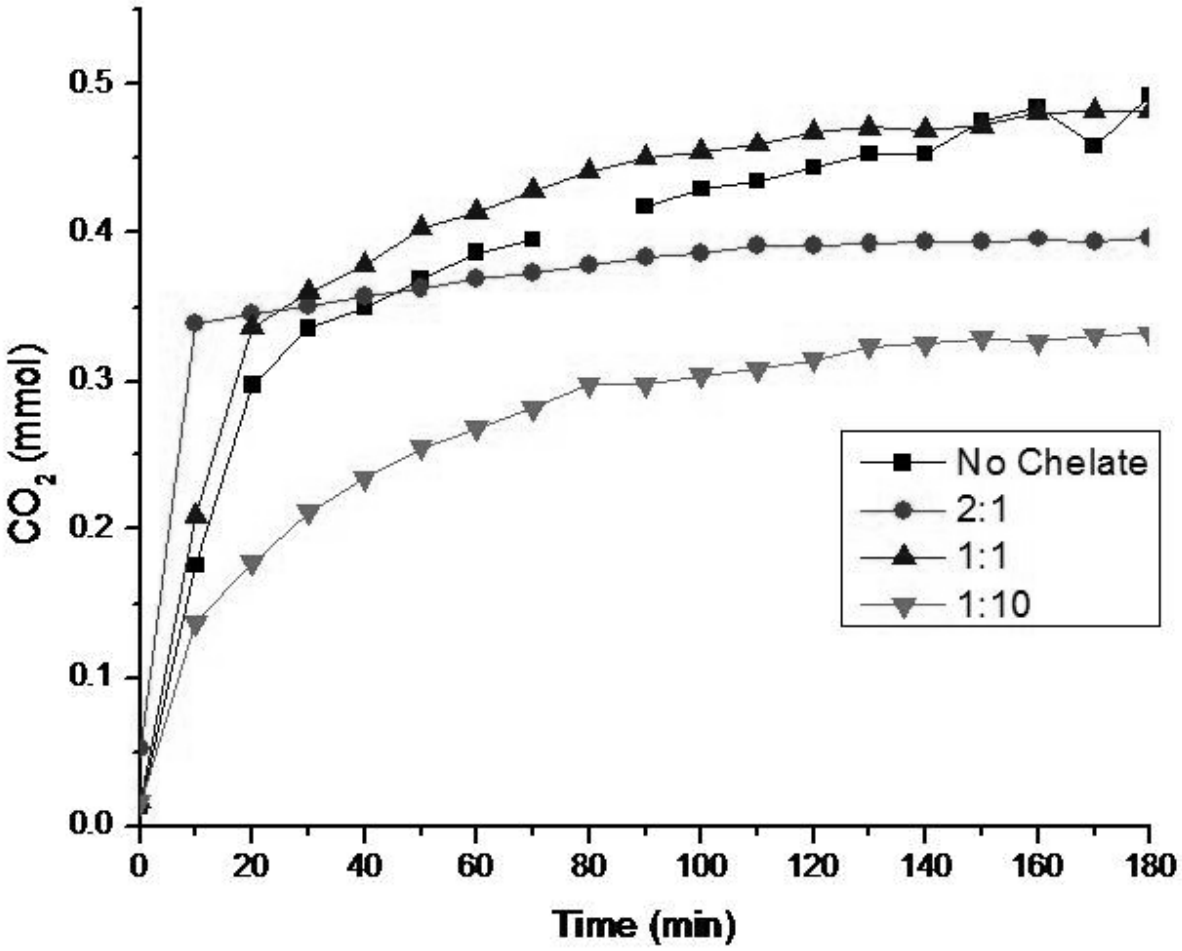

Figure 2-6 The production of CO_2 by the cobalt doped aerogels is shown above. All four aerogels produced less than 15% of the theoretical 3.56 mmol possible. Visible light exposure began at 120 minutes but resulted in no change of the production of CO_2.

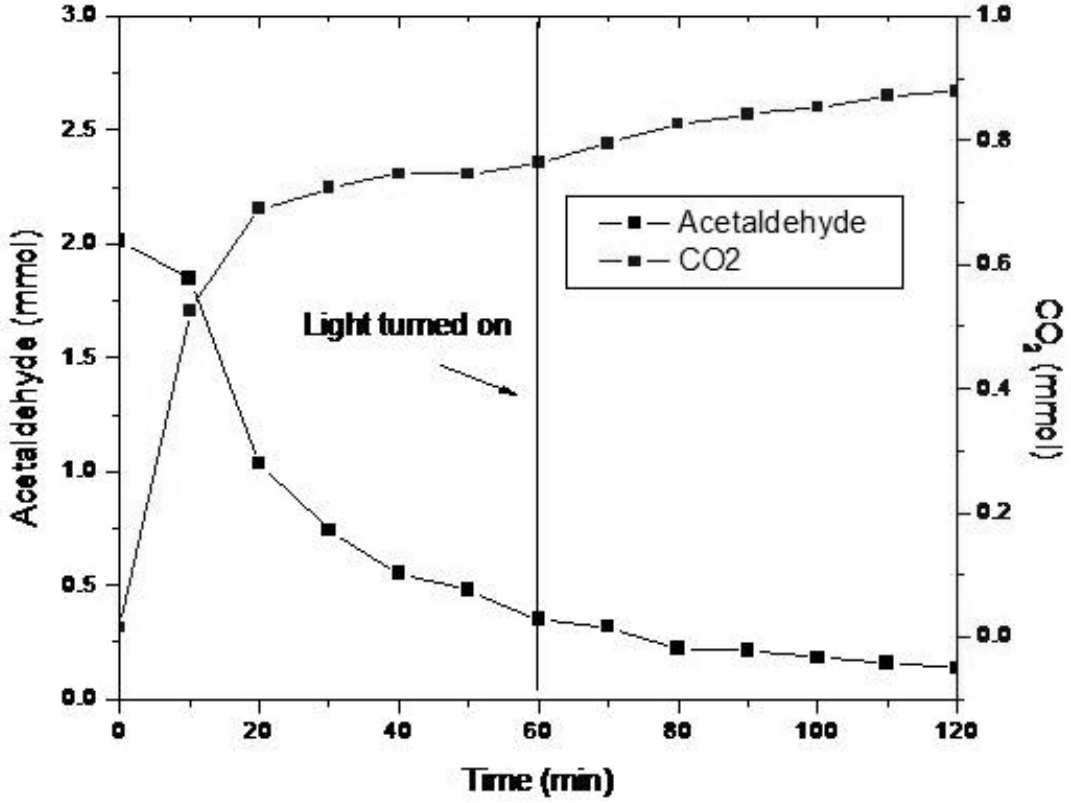

Figure 2-7 A 200 µL acetaldehyde experiment with exposure to visible light was performed using 100 mg of a powdered cobalt doped titania/silica aerogel. The resulting graph was subjected to a linear trendline examination from 50 minutes to 90. Based on the resulting trendline there is no statistical difference in the removal of acetaldehyde or production of CO_2 with the addition of visible light exposure.

To assess the effect of visible light on the cobalt doped system an experiment using 200 µL of acetaldehyde was monitored via GC-MS. GC-MS monitoring began immediately upon the introduction of acetaldehyde to the reactor vessel and the visible light was turned on at 60 minutes. As shown in **Figure 2-7**, the introduction of visible light to the system made no significant changes to the system or yields. A study was performed to test the effects of ultraviolet light on a system containing the cobalt doped aerogel with 100 µL of acetaldehyde. This experiment was allowed to come to equilibrium for 40 minutes before GC-MS monitoring

began; this and another test showed that ultraviolet light had no significant impact on the degradation of acetaldehyde or the production of CO_2.

The adsorption of acetaldehyde generally follows the trend with surface area. The initial concentration of acetaldehyde for the catalyst synthesized using a chelate ratio of 1:10 was a bit low but in the end the total removal of acetaldehyde is right on par. If the liquid acetaldehyde was not vaporized completely then the concentration would appear low via the GC-MS and since samples were only taken every 10 minutes it is possible the highest concentration of acetaldehyde was during a period not monitored.

2.10 Conclusions

A novel material based on a titania/silica system doped with 10 mol % cobalt was synthesized using the sol-gel method. It was treated in an autoclave (supercritical drying) to produce an aerogel with high surface area (200-300 m2/g). The catalysts showed absorption in the visible range but when exposed to visible and UV-light the material's activity was not increased. The base dark catalytic activity of the mixed metal oxide was quite impressive even without the enhancement from light. The overall degradation of all systems exceeded 95% of the total concentration of acetaldehyde and the production of CO2 was < 15% of the theoretical yield based on the initial concentration of acetaldehyde.

2.11 References

(1) Kesselmeier, J.; Staudt, M. Biogenic volatile organic compounds (VOC): an overview on emission, physiology and ecology. *J. Atmos. Chem.* **1999**, *33*, 23-88.

(2) Schauer, J. J.; Kleeman, M. J.; Cass, G. R.; Simoneit Bernd, R. T. Measurement of emissions from air pollution sources. 4. C1-C27 organic compounds from cooking with seed oils. *Environ Sci Technol* **2002**, *36*, 567-575.

(3) Schauer, J. J.; Kleeman, M. J.; Cass, G. R.; Simoneit, B. R. T. Measurement of Emissions from Air Pollution Sources. 3. C1-C29 Organic Compounds from Fireplace Combustion of Wood. *Environ. Sci. Technol.* **2001**, *35*, 1716-1728.

(4) Schauer, J. J.; Kleeman, M. J.; Cass, G. R.; Simoneit, B. R. T. Measurement of Emissions from Air Pollution Sources. 1. C1 through C29 Organic Compounds from Meat Charbroiling. *Environ. Sci. Technol.* **1999**, *33*, 1566-1577.

(5) US EPA, An Introduction to Indoor Air Quality (IAQ). *http://www.epa.gov/iaq/voc.html* (accessed 08/03, 2011).

(6) Zhao, X. S.; Ma, Q.; Lu, G. Q. VOC Removal: Comparison of MCM-41 with Hydrophobic Zeolites and Activated Carbon. *Energy Fuels* **1998**, *12*, 1051-1054.

(7) Heiderscheidt, J. L.; Crimi, M.; Siegrist, R. L.; Singletary, M. A. Optimization of full-scale permanganate ISCO system operation: laboratory and numerical studies. *Ground Water Monit. Rem.* **2008**, *28*, 72-84.

(8) Fujishima, A.; Honda, K. Electrochemical photolysis of water at a semiconductor electrode. *Nature (London)* **1972**, *238*, 37-38.

(9) Demydov, D.; Klabunde, K. J. Characterization of mixed metal oxides (SrTiO3 and BaTiO3) synthesized by a modified aerogel procedure. *J. Non-Cryst. Solids* **2004**, *350*, 165-172.

(10) Hamal, D. B.; Klabunde, K. J. Synthesis, characterization, and visible light activity of new nanoparticle photocatalysts based on silver, carbon, and sulfur-doped TiO2. *J. Colloid Interface Sci.* **2007**, *311*, 514-522.

(11) Yang, X.; Cao, C.; Hohn, K.; Erickson, L.; Maghirang, R.; Hamal, D.; Klabunde, K. Highly visible-light active C-doped and V-doped TiO2 for degradation of acetaldehyde. *J. Catal.* **2007**, *252*, 296-302.

(12) Kapoor, P. N.; Heroux, D.; Mulukutla, R. S.; Zaikovskii, V.; Klabunde, K. J. High surface area homogeneous nanocrystalline bimetallic oxides obtained by hydrolysis of bimetallic μ-oxo alkoxides. *J. Mater. Chem.* **2003**, *13*, 410-414.

(13) Kapoor, P. N.; Uma, S.; Rodriguez, S.; Klabunde, K. J. Aerogel processing of MTi2O5 (M=Mg, Mn, Fe, Co, Zn, Sn) compositions using single source precursors: synthesis, characterization and photocatalytic behavior. *J. Mol. Catal. A: Chem.* **2005**, *229*, 145-150.

(14) Kalebaila, K. K.; Klabunde, K. J. An inorganic oxide TiO2-SiO2-Mn aerogel for visible-light induced air purification. *ACS Symp. Ser.* **2010**, *1045*, 207-223.

(15) Hamal, D. B.; Klabunde, K. J. Valence State and Catalytic Role of Cobalt Ions in Cobalt TiO2 Nanoparticle Photocatalysts for Acetaldehyde Degradation under Visible Light. *J. Phys. Chem. C* **2011**, *115*, 17359-17367.

(16) Hench, L. L.; Wilson, M. J. R. Processing of gel-silica monoliths for optics. Drying behavior of small pore gels. *J. Non-Cryst. Solids* **1990**, *121*, 234-243.

(17) Hench, L. L.; West, J. K. The sol-gel process. *Chem. Rev.* **1990**, *90*, 33-72.

(18) Cushing, B. L.; Kolesnichenko, V. L.; O'Connor, C. J. Recent Advances in the Liquid-Phase Syntheses of Inorganic Nanoparticles. *Chem. Rev. (Washington, DC, U. S.)* **2004**, *104*, 3893-3946.

Chapter 3 - Degradation Studies of Semivolatile Organic Compounds (SVOCs) Using Titania/Silica Doped Photocatalysts

3.1 Introduction

There has been tremendous previous research focused on the environmental implications and degradation of volatile organic compounds (VOCs), inorganic gaseous pollutants, and airborne particles but semivolatile organic compounds (SVOCs) have received considerably less attention. This does not mean that they are any less important than other pollutants, rather they are challenging to analytically study due to difficulties in measurement. A semivolatile organic compound is defined as an organic molecule which has meaningful abundance in both the gas phase and condensed phases.[1] SVOCs span a wide range of vapor pressure ranging from 10^{-14} to 10^{-4} atm or 10^{-9} to 10 Pa. These pressures correspond to saturated mixture ratios of 0.01 ppt to 100 ppm in 1 atm of air. These compounds occur in both the outdoor and indoor environment.[1] As our society continues to evolve and technology takes a larger and larger role, more people find their working environment to be indoors. For this reason we must try and change the way people think about the world that they live in. For example, people do not typically think of pollution indoors but yet if you were to speak of pollution in a closed system versus an open system most would recognize the difference. The EPA has over 1000 SVOCs listed as high-production- volume (HPV).[2]

While shifting from volatile organic compounds to semivolatile organic compounds it was important to take into account what had already been observed. High surface area materials have shown better adsorption and degradation of volatile organic compounds.[3,4,5,6] Therefore when choosing which catalyst to use, it was important to include compounds based on titanium dioxide and silicon dioxide particularly aerogels. The higher surface area materials are able to trap more

molecules inside the interstitial space as well as bring the guest molecules into closer proximity of the reactive sites for degradation.

Our research began by studying disperse red 19 (DR19) as a model pollutant. DR19 was chosen because it is a well known dye which has a UV adsorption that can easily be monitored by UV-Vis for various reactions. Based on previous work with the various catalysts to be used in this series of experiments, it was hypothesized that they would act as good adsorbents and potentially even have the capability of degrading DR19.The initial goals were to establish a method for detecting SVOCs in the liquid phase and provide meaningful data for establishing novel indoor air remediation. Previous work has focused on the use of high surface area catalysts for the degradation of VOCs in the gas phase. These reactions are easily monitored using GC/MS via the detection of the CO_2 gas product. SVOCs on the other hand are less volatile meaning their concentrations in the gas phase will be too small to quantify.

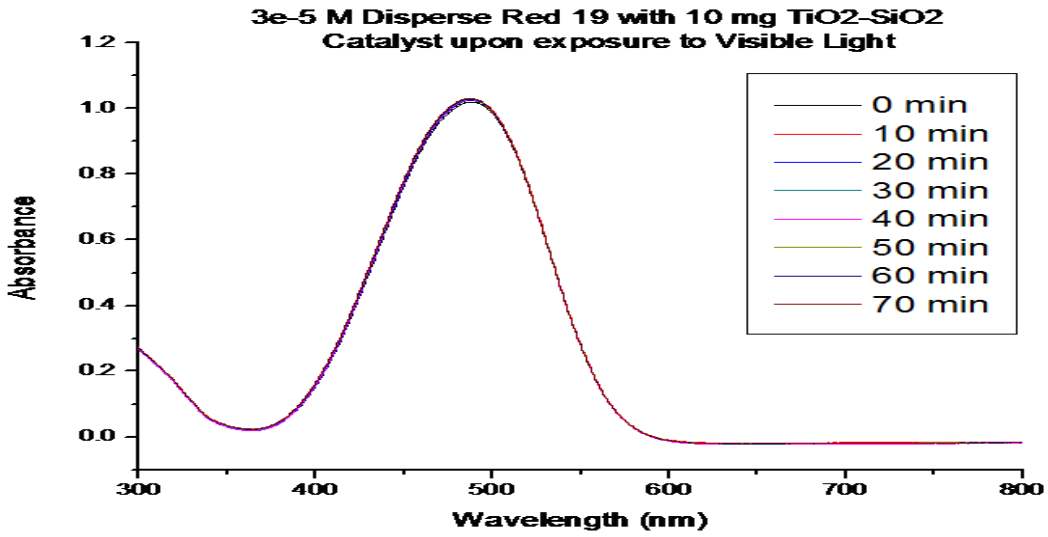

Figure 3-1 Shown here is DR19 in THF during a visible light irradiation. THF is a polar solvent which prevents interactions between the catalyst and DR19.

It is for this reason we opted to use liquid phase reactions to mimic the interactions between the catalyst and the pollutant. The choice of solvent is very important for these types of reactions for reasons such as potential UV-Vis peak overlap and solubility of the pollutant and catalysts. For the initial testing of DR19 tetrahydrofuran, THF was used as the solvent as it is known to work well with DR19. The testing of DR19 dissolved in THF concluded that the solvent was holding onto the DR19 too tightly preventing interactions between DR19 and the catalysts. The catalyst TiO_2/SiO_2 was not able to react with the pollutant as shown in **Figure 3-1**. After reviewing the available solvent choices, toluene was chosen as it is a less polar solvent it is more likely to allow for the pollutant to interact with the catalyst. The hope was that only the interactions between the pollutant and the catalyst would dominate and the solvent-pollutant interactions would be quenched.

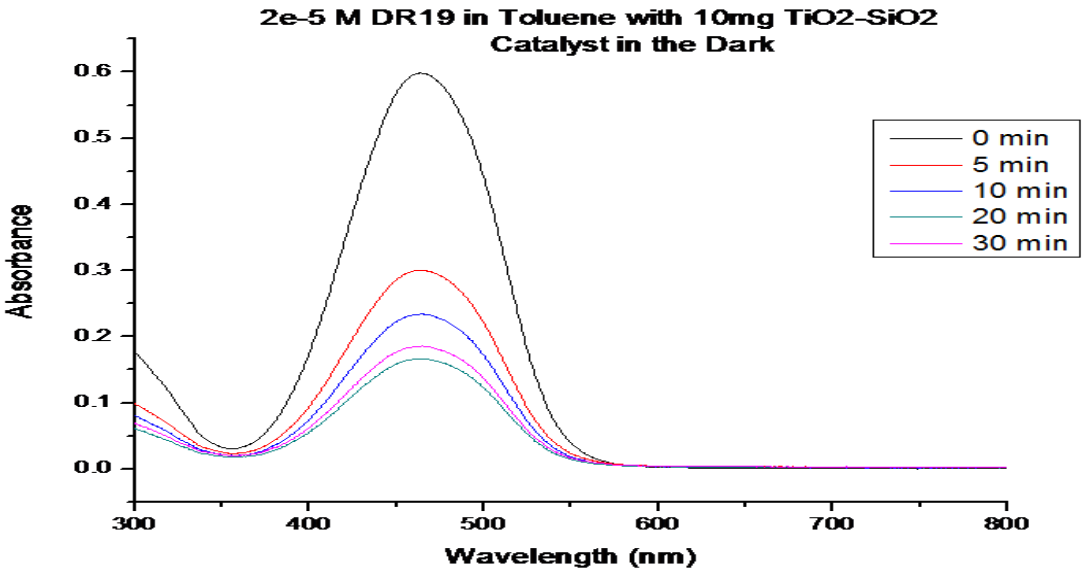

Figure 3-2 Shown here is the UV-Vis of visible light irradiated DR19 dissolved in toluene. Toluene is less polar than THF and allows for the interaction of catalyst and pollutant.

When toluene was used, it was found that DR19 did dissolve well and the reactions in solution showed promising results as shown above in **Figure 3-2**. Typical reactions used 100 mL of 2.0 X 10^{-5} M DR19 in toluene with 10 mg of catalyst. These reactions were carried out at room temperature in a closed container. The reactions were monitored using UV-Vis spectroscopy which required the liquid samples to be centrifuged to remove any solid catalyst. Several different catalysts were tested via this method using three different methods: no irradiation, visible light irradiation and ultraviolet light irradiation.

3.2 Experimental

Typically gas phase reactions are preferred because they can easily be monitored by gas chromatography/mass spectroscopy. This works well for volatile organic compounds as they are present in the gas phase in large enough concentrations to measure. Semivolatile organic compounds on the other hand by nature are present in very low concentrations in the gas phase. For this reason ultra-violet adsorption spectroscopy is the method of choice for monitoring reactions of semivolatile organic compounds with the various catalysts.

Liquid phase reactions were carried out in a closed system using a round bottom flask with a septum. These reactions were performed in the absence of light. Triphenyl phosphate, an SVOC, was dissolved in various solvents: tetrahydrofuran, toluene and n-pentane to find the optimal peak resolution using ultra-violet adsorption. The following procedure is a general overview of those experiments. Triphenyl phosphate was dissolved in n-pentane to achieve a molarity of 10^{-3}M. 100 mL of triphenyl phosphate in n-pentane was placed in a 250 mL round bottom flask. Then 10 mg of varying catalysts was added to the round bottom flask and capped with a rubber septum. This mixture was stirred vigorously throughout the duration of the experiment. At given intervals ca. 5 mL aliquot samples were centrifuged at 8000 rpm for 2

minutes and subjected to ultra-violet adsorption spectroscopy using a Cary 500 UV-Vis spectrophotometer.

To test the catalysts for photodegradation of semivolatile organic compounds, triphenyl phosphate dissolved in n-pentane was placed in a 305 mL cylindrical air-filled glass reactor with a quartz window. The reactor was maintained at room temperature using a water jacket. A stir bar and 10 mg of varying catalysts were added to the reactor. Upon sealing the reactor it was irradiated using a 1000 W high-pressure mercury Oriel Corp. lamp. The light was filtered using a VIS-NIR long pass filter (400 nm) and a colored glass filter (>420 nm).

A real time monitoring ultra-violet adsorption instrument was discovered and was used in hopes of obtaining more accurate data. After several attempts with this instrument and using the different solvents it was concluded that the instrument was unable to perform analysis in the UV range needed which is roughly 270 nm and below.

3.3 Results

Based on the previous research performed by the REU student Jackie Johnson, it was clear that finding the proper solvent was the first challenge for using a new model pollutant. Therefore several solvents were tested before settling on n-pentane. The first solvent tested was THF which showed no changes in the UV spectra as the concentration of triphenyl phosphate changed. The second solvent used was toluene. It was believed that the solvent would interfere with the absorbance of triphenyl phosphate since they would both be in the UV range but we wanted to be sure since toluene had worked well for DR19. Upon testing of triphenyl phosphate in toluene it was concluded to be true. The third solvent choice was n-pentane. N-pentane was thought to be the best choice based on the previous research results due to its nature as a non-polar solvent. It was found using DR19 that solvent interactions are a key problem when trying

to perform liquid phase reactions with our catalysts and particularly less polar solvents were more effective.

After obtaining standards of varying concentrations of triphenyl phosphate in n-pentane (**Figure 3-3**), reactions were carried out with solutions of 100 mL of 10^{-3} M and 10 mg of varying catalyst. For this series of reactions various titanium dioxide and silicon dioxide based catalysts were used and it was therefore prudent to use P25 Degussa as a standard reference. Another material used as a comparison point was sol-gel prepared titanium dioxide-silicon dioxide. This catalyst was synthesized using supercritical drying to obtain a high surface area aerogel. These two materials acted as references for the doped catalysts used later.

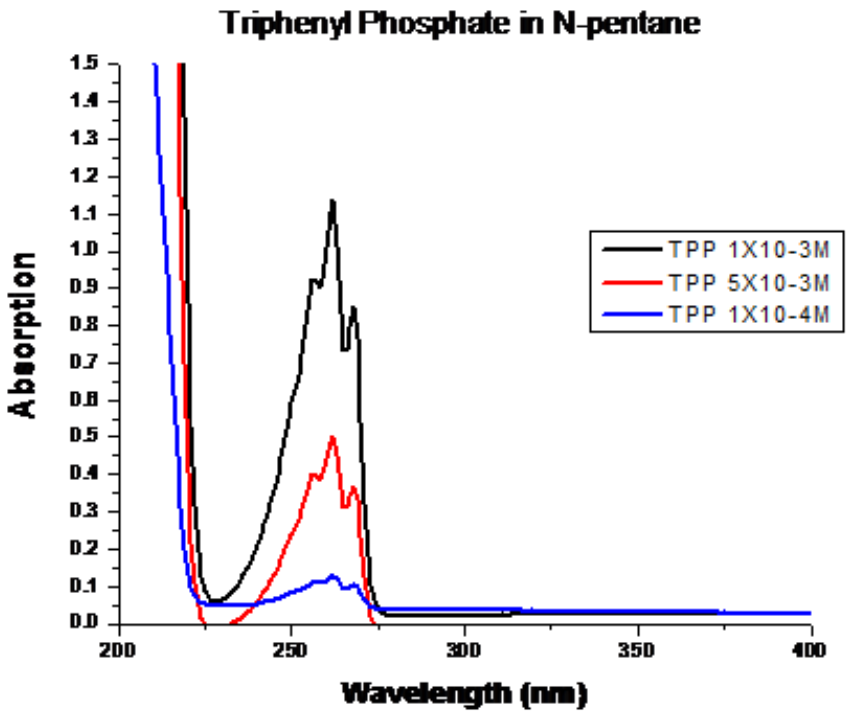

Figure 3-3 Triphenyl phosphate (TPP) dissolved in n-pentane is able to be monitored using UV-Vis at varying concentrations as shown above.

The non-irradiated reactions of triphenyl phosphate in n-pentane with P25 Degussa and the sol-gel prepared titanium dioxide- silicon dioxide showed no significant adsorption of the triphenyl phosphate from solution after 16 hours as shown in **Figure 3-4**. A manganese doped variation of the titanium dioxide-silicon dioxide catalyst showed a peculiar trend as the time of reaction increased. A comparison of the varying catalysts is shown in **Figure 3-5**.

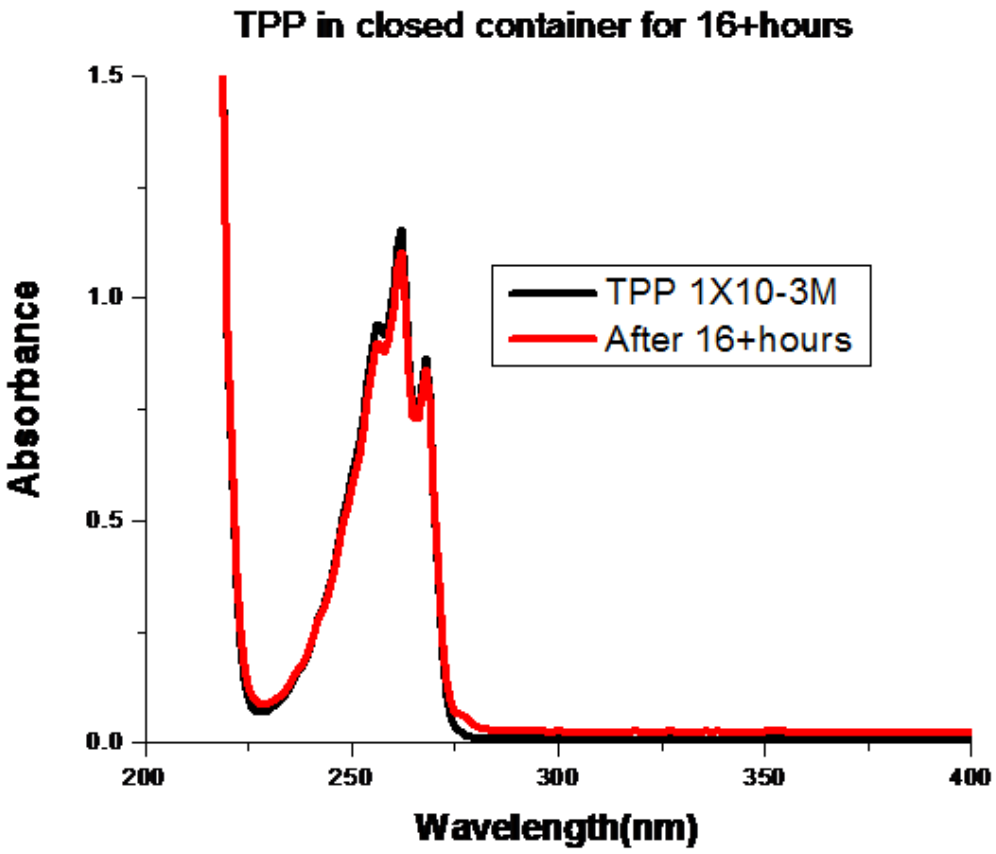

Figure 3-4 A catalyst made of titanium dioxide-silicon dioxide prepared by the sol-gel method has been reacted with triphenyl phosphate for over 16 hours and the concentration of the pollutant has remained the same.

As shown in **Figure 3-5**, the manganese doped catalyst exhibits a strange behavior. Instead of the peaks associated with triphenyl phosphate decreasing, which would indicate a change in the concentration, the peaks begin to grow with time. Also a new broad peak begins to form indicating the presence of a new compound. To determine the nature of this compound the liquid phase and solvent were extracted and examined using thin layer and flash chromatography. Using thin layer chromatography, three different samples were analyzed: stock solution of triphenyl phosphate dissolved in n-pentane, the solution after reaction and a mixture of both. After allowing TLC plate time in solution the plated was checked for separation of compounds by diffusion. It was found that the sample of solution after the reaction contained new spots indicating compounds not found in the triphenyl phosphate stock solution.

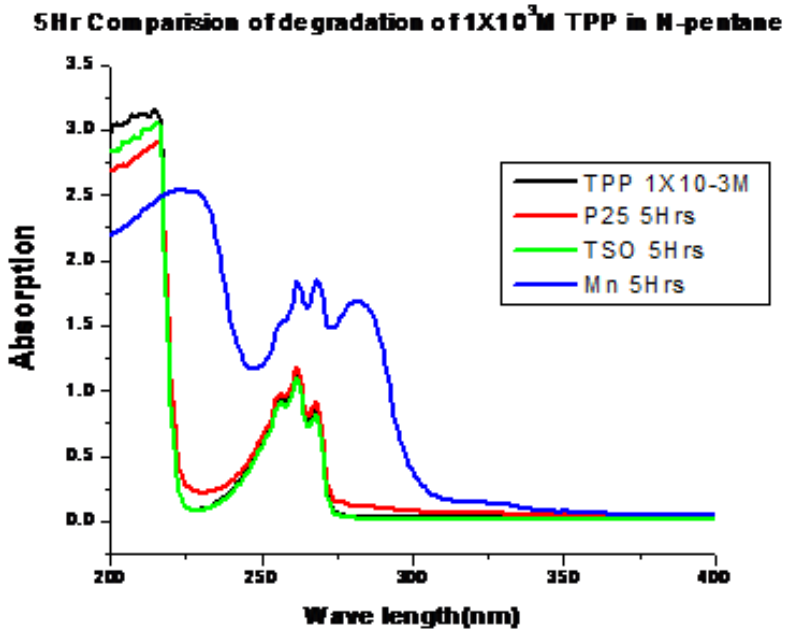

Figure 3-5 A 5 hr comparison of reactivity of P25, titanium dioxide-silicon dioxide and manganese doped titanium dioxide-silicon dioxide is shown. After 5 hrs only the manganese doped catalyst has shown any changes.

A sample of the solid manganese doped catalyst was analyzed by solid UV-Vis diffuse reflectance using a Cary 500 UV-Vis spectrometer. The sample was also analyzed using IR spectroscopy. In both cases the solid catalyst had slight changes in the before and after.

3.4 Conclusions

The liquid phase reactions have shown that catalysts must be tailored to the pollutant in which they are intended to degrade. This also holds true for the adsorption of pollutants onto surface sites of sorbents as reflected in the lack of adsorption shown in these studies. The manganese 10 mol % doped titania/silica catalyst showed a peculiar activity, where the peaks of the triphenyl phosphate increased and a new broad shoulder appeared red shift from those peaks. This indicates that the manganese catalyst is participating in some form of reaction but these products were unable to be separated for independent analysis due to polar proximity to triphenyl phosphate which limits the use of choromatography as a separating method.

3.5 References

(1) Weschler, C. J.; Nazaroff, W. W. Semivolatile organic compounds in indoor environments. *Atmos. Environ.* **2008**, *42*, 9018-9040.

(2) US EPA High Production Volume (HPV) Challenge. *http://www.epa.gov/chemrtk/index.htm*2010).

(3) Hamal, D. B.; Klabunde, K. J. Valence State and Catalytic Role of Cobalt Ions in Cobalt TiO2 Nanoparticle Photocatalysts for Acetaldehyde Degradation under Visible Light. *J. Phys. Chem. C* **2011**, *115*, 17359-17367.

(4) Hamal, D. B.; Klabunde, K. J. Synthesis, characterization, and visible light activity of new nanoparticle photocatalysts based on silver, carbon, and sulfur-doped TiO2. *J. Colloid Interface Sci.* **2007**, *311*, 514-522.

(5) Kalebaila, K. K.; Klabunde, K. J. An inorganic oxide TiO2-SiO2-Mn aerogel for visible-light induced air purification. *ACS Symp. Ser.* **2010**, *1045*, 207-223.

(6) Kapoor, P. N.; Uma, S.; Rodriguez, S.; Klabunde, K. J. Aerogel processing of MTi2O5 (M=Mg, Mn, Fe, Co, Zn, Sn) compositions using single source precursors: synthesis, characterization and photocatalytic behavior. *J. Mol. Catal. A: Chem.* **2005**, *229*, 145-150.